© 2020. Published by The Company of Biologists Ltd | Development (2020) 147, dev184044. doi:10.1242/dev.184044

STEM CELLS AND REGENERATION

RESEARCH ARTICLE

Planarian cell number depends on *blitzschnell*, a novel gene family that balances cell proliferation and cell death

Eudald Pascual-Carreras[1,2], Marta Marin-Barba[3], Carlos Herrera-Úbeda[1,2], Daniel Font-Martín[1,2], Kay Eckelt[1,2], Nidia de Sousa[1,2], Jordi García-Fernández[1,2], Emili Saló[1,2] and Teresa Adell[1,2,*]

ABSTRACT

Control of cell number is crucial to define body size during animal development and to restrict tumoral transformation. The cell number is determined by the balance between cell proliferation and cell death. Although many genes are known to regulate those processes, the molecular mechanisms underlying the relationship between cell number and body size remain poorly understood. This relationship can be better understood by studying planarians, flatworms that continuously change their body size according to nutrient availability. We identified a novel gene family, *blitzschnell* (*bls*), that consists of *de novo* and taxonomically restricted genes that control cell proliferation: cell death ratio. Their silencing promotes faster regeneration and increases cell number during homeostasis. Importantly, this increase in cell number leads to an increase in body size only in a nutrient-rich environment; in starved planarians, silencing results in a decrease in cell size and cell accumulation that ultimately produces overgrowths. *bls* expression is downregulated after feeding and is related to activity of the insulin/Akt/mTOR network, suggesting that the *bls* family evolved in planarians as an additional mechanism for restricting cell number in nutrient-fluctuating environments.

KEY WORDS: Body size, Cell number, Growth, Regeneration, Overgrowth, mTOR

INTRODUCTION

During embryonic development, all species undergo dramatic increases in size until reaching a definitive body size, which is strikingly similar across species. The definitive body size of an organism is reached by increasing either cell number or cell size. Changes in cell size have been described in specific organs, e.g. imaginal discs in *Drosophila* (Miyaoka et al., 2012; Hariharan, 2015). However, regulation of cell number, achieved by modulating the balance between cell death and cell proliferation, is the main mechanism by which animals reach their definitive body size (Guertin and Sabatini, 2006). Although conceptually simple, the developmental mechanisms that control cell number constitute one of the more intriguing issues in biology. In general, the main signaling pathways thought to control growth regulate cell proliferation and cell death in response to the nutritional environment. Studies in multiple species have identified the same key signaling pathways that appear to regulate body size: the JNK pathway, the Hippo pathway and the insulin/Akt/mTOR signaling network. The JNK signaling pathway controls cell death and proliferation, mainly in response to cellular stress (Dhanasekaran and Reddy, 2017). The Hippo signaling pathway regulates proliferation, apoptosis and cell differentiation in response to mechanical stimuli (Udan et al., 2003; Zeng and Hong, 2008). Genetic perturbation of JNK or Hippo signaling leads to overgrowths or organ size changes, but does not affect overall body size (Tumaneng et al., 2012; Willsey et al., 2016). In contrast, activation of the insulin/Akt/mTOR signaling network leads to increases in body size in animals as distant as *Drosophila* and mice (Saxton and Sabatini, 2017). Insulin/Akt/mTOR signaling is the most conserved molecular mechanism that relates nutrient intake to cell proliferation (Gokhale and Shingleton, 2015), and it is the main regulator of cell size in response to cellular amino acid levels (González and Hall, 2017; Wolfson and Sabatini, 2017).

The study of planarians, flatworms that display extraordinary cell plasticity, can help further our understanding of the molecular mechanisms that control body size during development. In most animals, adult body size is determined by growth during embryonic and juvenile stages, while the adult stage consists of tissue renewal. However, long-living species, such as planarians, change their body size according to nutrient availability during their entire lives. These alterations in planarian body size are mediated by changes in cell number (Baguñá and Romero, 1981; Thommen et al., 2019) resulting from modulation of the balance between cell proliferation and apoptosis. Thus, the ratio of proliferation to apoptosis decreases in starvation conditions and increases in times of nutritional abundance (Baguñá, 1976; Pellettieri et al., 2010). Planarian plasticity is sustained by a population of pluripotent adult stem cells (neoblasts) that can differentiate into any planarian cell type. Furthermore, the balance between the stem cell population and all types of differentiated cells relies on robust signaling mechanisms that allow continuous adjustment of cell proliferation, cell death and cell differentiation. The signaling pathways that determine cell fate and tissue patterning in planarians, including the Wnt and BMP pathways, have been extensively studied (Molina et al., 2011; Sureda-Gómez et al., 2016). However, the mechanisms that control planarian body size and growth remain to be fully elucidated. The insulin/mTOR pathway is the only pathway demonstrated to control planarian body size. Inhibition of insulin-like peptides or TOR attenuates cell proliferation, prevents planarian growth after feeding and accelerates shrinking during starvation (Miller and Newmark, 2012; Tu et al., 2012). Hyper-activation of mTOR using *PTEN* or *smg-1* RNA interference (RNAi) does not give rise to larger organisms but does promote overproliferation and outgrowth formation (Oviedo et al., 2008; González-Estévez et al., 2012a,b). In planarians, *JNK* is required for organ remodeling through the

[1]Department of Genetics, Microbiology and Statistics and Institute of Biomedicine, Universitat de Barcelona, Barcelona 08028, Catalunya, Spain. [2]Institut de Biomedicina de la Universitat de Barcelona (IBUB), Universitat de Barcelona, Barcelona 08028, Catalunya, Spain. [3]School of Biological Sciences, University of East Anglia, Norwich Research Park, Norwich NR4 7TJ, UK.

*Author for correspondence (tadellc@ub.edu)

E.P.-C., 0000-0002-9577-840X; C.H.-Ú., 0000-0002-2334-9470; N.d.S., 0000-0002-1895-9530; T.A., 0000-0002-5446-1510

Received 20 August 2019; Accepted 19 February 2020

Development (2020) 147, dev184044. doi:10.1242/dev.184044

induction of apoptotic cell death (Almuedo-Castillo et al., 2014). Moreover, *hippo* inhibition increases mitosis, inhibits apoptosis and promotes dedifferentiation, leading to the formation of overgrowths but not to changes in body size or cell number (de Sousa et al., 2018). Planarian plasticity not only facilitates adaptation to the environment but also enables reproduction: most species reproduce asexually through fissioning the tail, producing two segments from which two complete organisms regenerate. Amputation in planarians triggers tightly controlled apoptotic and mitotic responses (Baguñá and Salo, 1984; Pellettieri et al., 2010; Wenemoser and Reddien, 2010). Silencing of several signaling pathways, such as the JNK or TOR pathways, results in the formation of smaller blastemas in which cell proliferation, apoptosis and/or differentiation is impaired (Peiris et al., 2012; Tu et al., 2012; Almuedo-Castillo et al., 2014). Interestingly, TOR hyper-activation gives rise to larger blastemas, although they remain undifferentiated (González-Estévez et al., 2012a,b), and Hippo hyper-activation enhances the wound response, promoting the expansion of cell populations (Lin and Pearson, 2017).

Here, we describe the identification of a novel gene family that we have named *blitzschnell* (*bls*), which controls cell proliferation and cell death in intact and regenerating planarians. The *bls* family consists of 11 genes and four pseudogenes that can be classified into five subfamilies (*bls1-bls5*). The family is composed of *de novo* genes, which appear to be taxonomically restricted to the order Tricladida (commonly known as planarians). Silencing of *bls2/bls3/bls5* promotes faster regeneration and increases cell number during homeostasis. However, this increase in cell number leads to an increase in body size only in nutrient-rich environments: during starvation cells are unable to maintain their normal size and become smaller than those of control animals. Importantly, expression of *bls2*, *bls3* and *bls5* is downregulated after nutrient intake, and it was found to be related to the insulin/Akt/mTOR network, suggesting that in planarians the *bls* family may have evolved as an additional mechanism to restrict cell number in nutrient-fluctuating environments.

RESULTS

blitzschnell is a new gene family organized in two clusters of tandem repeats in *Schmidtea mediterranea*

We performed an RNAi screen to find candidate genes involved in planarian eye regeneration, and identified an unknown gene whose inhibition resulted in faster regeneration of the eyes after head amputation. We named this gene *blitzschnell* (*bls*), which means ‘quick as a flash’ in German. Surprisingly, upon attempting to identify the genomic locus of this gene in *Schmidtea mediterranea*, we found that *bls* belongs to a gene family composed of 15 members distributed on two distinct genomic scaffolds (Fig. 1A, Table S1).

Although all *bls* sequences shared more than 70% identity (Table S2), a phylogenetic analysis using the nucleotide sequence allowed us to classify *bls* genes into five subfamilies (Fig. S1A). Four of these subfamilies (*bls1*, *bls2*, *bls4* and *bls5*) contained two putative genes each (named a and b), apparently derived from duplications. Subfamily *bls3* contained seven *bls* sequences (named *bls3a-bls3g*). These were also apparently derived from recent successive tandem duplications, as suggested by their genomic organization (Fig. 1A) and near identical DNA sequences (Table S1; Table S2). One band of the expected size was successfully amplified using primers spanning the junction between *bls3a* and *bls3b*, confirming the existence of at least two repeats (Fig. 1A, Fig. S1B, Table S3). Interestingly, in the repeated block harboring *bls3* members and in the vicinity of other *bls* genes, we identified complete or fragmentary transposon-related genes, including the genes encoding the reverse transcriptase RNAse H and integrase (Fig. 1A).

By mapping reads from the transcriptome of intact planarians (de Sousa et al., 2018) against the genome of *S. mediterranea* (Grohme et al., 2018), we detected transcripts for subfamilies *bls2*, *bls3* and *bls5,* but not for subfamilies *bls1* or *bls4* (Fig. S1C). Furthermore, the predicted open reading frame (ORF) for *bls2*, *bls3* and *bls5* encoded peptides containing a N-terminal signal peptide (SP), suggesting that they could be secreted, and a highly conserved C-terminal coiled-coil (CC) domain (Fig. 1B, Table S4). Non-detectable transcription,

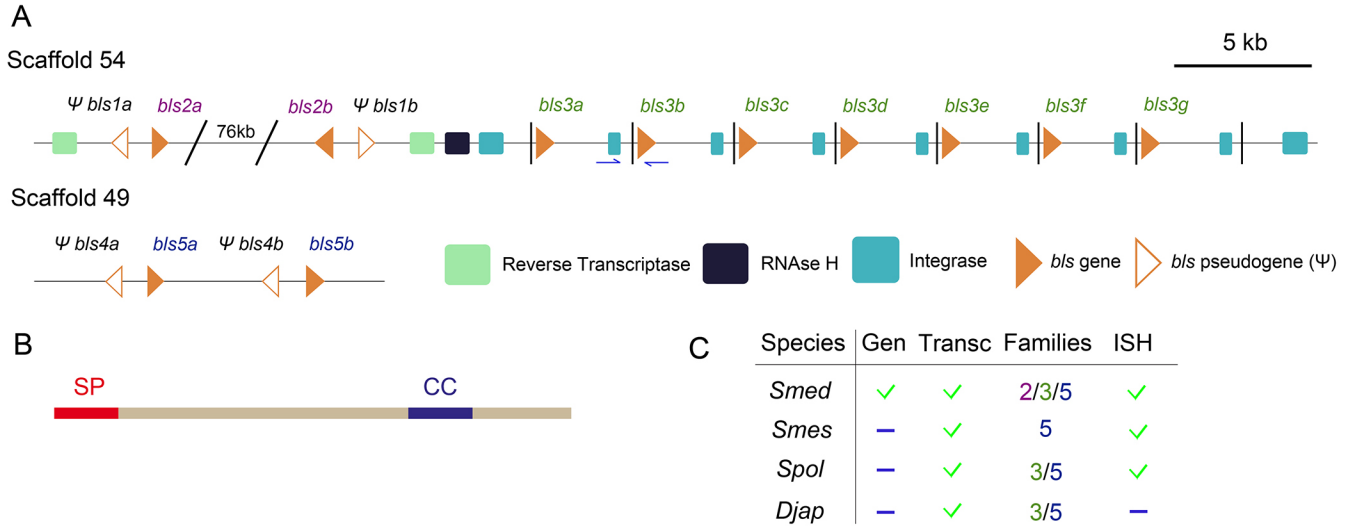

Fig. 1. The *bls* family is composed of 11 genes and four pseudogenes. (A) Cartoon illustrating the genomic organization of Bls family members. Subfamilies *bls1*, *bls2* and *bls3* are found in scaffold 54, and subfamilies *bls4* and *bls5* in scaffold 49. Primers used to amplify the junction of the first *bls3* repeats are indicated in blue. *bls* genes are represented by orange triangles. *bls* pseudogenes (Ψ) are represented by white and orange triangles. Transposon elements are indicated with squares. Scale bar indicates base pairs. (B) Bls protein domains: red, signal peptide (SP); blue, coiled coil (CC). (C) *bls* homologs found in the available genomic (Gen) and transcriptomic (Transc) datasets for planarian species. Expression as detected by *in situ* hybridization is indicated. Green tick indicates presence of *bls* homolog; blue line indicates no available data. ISH, *in situ* hybridization; *Smed*, *Schmidtea mediterranea* (asexual strain); *Smes*, *Schmidtea mediterranea* (sexual strain); *Spol*, *Schmidtea polychroa*; *Djap*, *Dugesia japonica*.

Development (2020) 147, dev184044. doi:10.1242/dev.184044

together with a much shorter ORF, strongly suggests that subfamilies *bls1* and *bls4* are made up of pseudogenes (Ψ).

Taken together, these data demonstrate that *bls* is a new gene family consisting of 11 genes and four pseudogenes. The genes encode very similar peptides that may be released into the extracellular space, as suggested by the presence of a signal peptide.

The *bls* family is taxonomically restricted to Tricladida

A BLAST search using *S. mediterranea bls* sequences against non-redundant transcriptomic and proteomic databases of all species (NCBI) produced no significant results. More-specific BLAST searches against genomic and transcriptomic datasets for Platyhelminth species (Egger et al., 2015) (NCBI and Planmine) indicated that homologs of the *bls* family are found only in species of the order Tricladida (planarians) (Fig. S1D; Table S5): *Schmidtea polychroa* (*Spol*), *Dugesia japonica* (*Djap*) and the sexual *S. mediterranea* strain (*Smes*). Although genomic databases are available for only a few Lophotrochozoa species, this result suggests that the *bls* family is taxonomically restricted to order Tricladida. Interestingly, a BLAST search of the available transcriptomic databases for Tricladida species returned more than one hit for those species (Fig. 1C), with a high degree of similarity at the nucleotide level (Table S6). Phylogenetic analysis performed with amino acid sequences (Table S7) revealed that the *bls5* subfamily was present in all Tricladida species studied; the *bls3* subfamily was present in *Smed*, *Spol*, and *Djap*; and the *bls2* subfamily was present only in *Smed* (Fig. 1C, Fig. S1E). However, it should be borne in mind that transcriptomic databases for Tricladida species other than *Smed* are incomplete. These findings suggest that the *bls* family is taxonomically restricted to Tricladida.

Subfamilies *bls2*, *bls3* and *bls5* are expressed in secretory cells

Although the three transcribed *bls* subfamilies (*bls2*, *bls3* and *bls5*) shared a high percentage of sequence identity at nucleotide level (Table S2), we designed riboprobes spanning different gene regions (Table S3, Table S8) to specifically detect genes from each subfamily. Whole-mount *in situ* hybridization with each riboprobe revealed the same pattern of expression and labelled specific dorsal-prepharyngeal cells (Fig. 2A, Fig. S2A). Double fluorescence *in situ* hybridization (FISH) revealed co-expression of genes from the three families in the same cells, although not presenting identical subcellular localization (Fig. S2B), confirming riboprobe specificity.

The *bls3* riboprobe revealed that *bls3*$^{+}$ cells were located dorsally and in the marginal cells throughout the body (Fig. 2A). These *bls3*$^{+}$ cells were differentiated, as they were insensitive to irradiation (Fig. S2C), and corresponded to secretory cells, as they co-expressed *dd4277*, a secretory and parenchymal cell marker (Fincher et al., 2018; Plass et al., 2018) (Fig. 2B). *bls3* was not expressed in blastemas during regeneration, but re-established its expression pattern according to the remodeling of the fragment in question (Fig. S2D). Interestingly, whole-mount *in situ* hybridization in sexual *S. mediterranea* (*Smes*) and *S. polychroa* (*Spol*) revealed the same expression pattern as observed for *Smed* (Fig. S2E), supporting a conserved function among Tricladida species (Fig. 1C). Taken together, our data indicate that genes from subfamilies *bls2*, *bls3* and *bls5* are expressed in a specific subpopulation of secretory prepharyngeal cells in planarians.

Inhibition of *bls* genes promotes faster regeneration

Because *bls2*, *bls3* and *bls5* genes share a high percentage of identity (Table S2), specific inhibition of any of these genes using RNAi was technically impossible. Furthermore, the high level of shared identity and cellular colocalization (Fig. S2B) suggested that at least some paralogs may perform similar functions. For this reason we designed double-stranded RNAs (dsRNAs) corresponding to a highly conserved region in order to inhibit genes of each of the three subfamilies (Fig. S3B, Table S8). qPCR analysis using primers specific to each subfamily (Fig. S3B) showed that expression levels of each of the three subfamilies were downregulated after RNAi (Fig. S3A,C). Sequencing of the fragments amplified by each qPCR corroborated inhibition of the genes of each of the three subfamilies (see Materials and Methods; Fig. S3C). These animals are referred to henceforth as *bls2/3/5*(RNAi) animals.

RNAi of *bls2*, *bls3* and *bls5* confirmed our initial observation of faster regeneration after head amputation in planarians. We observed earlier differentiation of the eye spots (Fig. S3D), and earlier differentiation of photoreceptor cells (identified by anti-arrestin immunostaining): after 3 days of regeneration (3dR, the optic chiasm was visible in most *bls2/3/5*(RNAi) animals but not in control animals (Fig. 3). In addition to the visual system, other anterior structures, such as the brain branches and chemoreceptors, regenerated faster than controls (Fig. 3), as evidenced by quantification of *gpas*$^{+}$ (Cebrià et al., 2002) and *cintillo*$^{+}$ (Oviedo et al., 2003) cells, respectively. Quantification of *pitx*$^{+}$ cells (Currie and Pearson, 2013; März et al., 2013) revealed an increase the

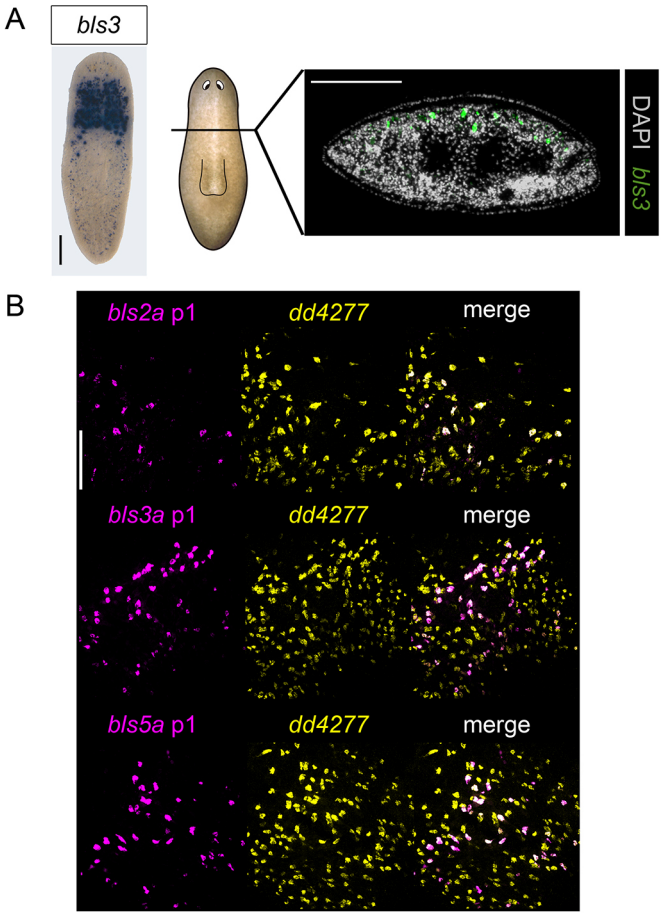

Fig. 2. *bls* expression pattern. (A) *bls3* expression in a transverse section, as detected by whole-mount *in situ* hybridization (blue) and fluorescent *in situ* hybridization (green). Nuclei are stained with DAPI. (B) *bls2*, *bls3* and *bls5* co-expression with *dd4277*. Scale bars: 200 µm.

Development (2020) 147, dev184044. doi:10.1242/dev.184044

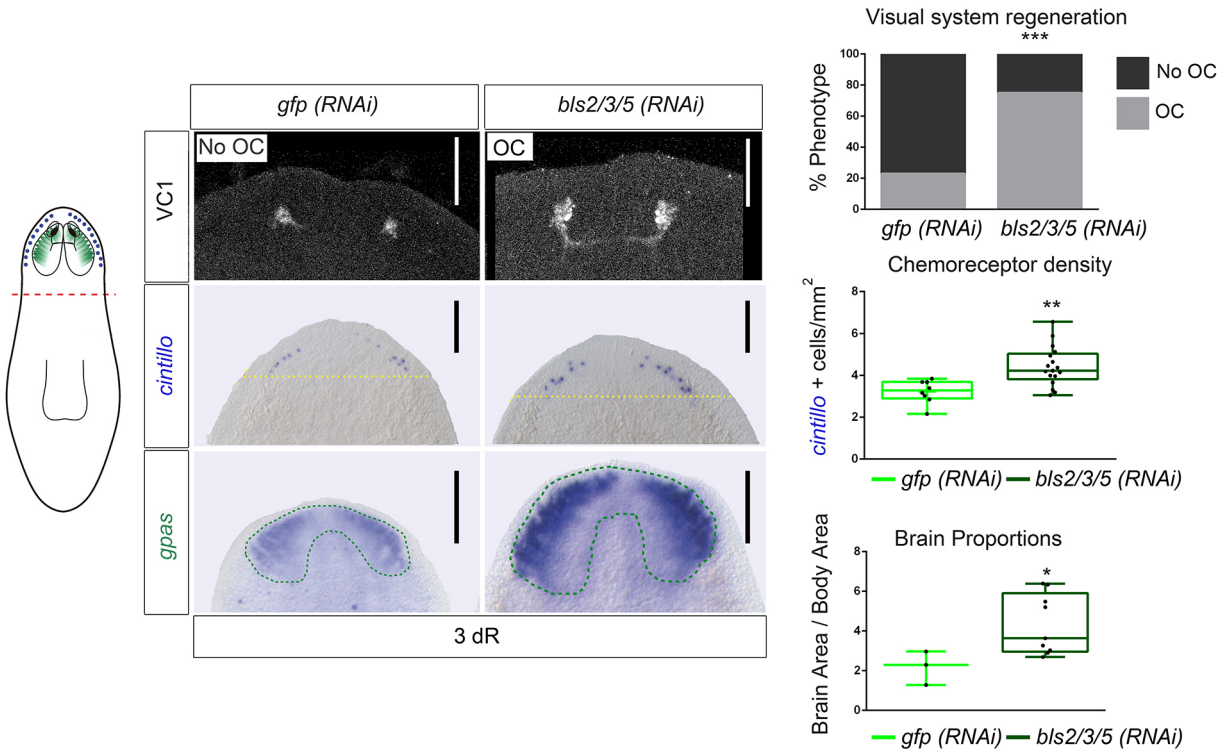

Fig. 3. Regeneration is accelerated in *bls2/3/5* RNAi planarians. Immunohistochemistry with anti-arrestin antibody (VC1), labelling the visual system; whole-mount *in situ* hybridization showing *cintillo* (chemoreceptors) and *gpas* (brain branches) expression. Illustration indicates areas of *gpas* and *cintillo* expression and positive arrestin (VC1) staining; dashed red line represents the level at which amputation was performed. Graphs show quantification of the appearance of the optic chiasm (controls, *n*=23; RNAi, *n*=23; ***P<0.001), *cintillo*$^+$ cells/mm^2 (the area quantified is indicated with a yellow dashed line) (controls, *n*=8; RNAi, *n*=17, **P<0.01) and *gpas*$^+$ area/body area (gpas$^+$ area is indicated with a green dashed line) (controls, *n*=3; RNAi, *n*=9 ;*P<0.05) in *gfp*(RNAi) and *bls2/3/5*(RNAi) animals at 3 days of regeneration (3 dR). Scale bars: 100 µm.

number of differentiated neural cells in the blastema of *bls2/3/5*(RNAi) planarians as early as 18 h of regeneration (hR) (Fig. S3E). These results demonstrate that inhibition of *Smed-bls2/3/5* promotes faster regeneration.

bls genes attenuate cell proliferation and promotes cell death after injury

To understand the mechanism by which *Smed-bls2/3/5*(RNAi) promotes faster regeneration, we analyzed the proliferative and apoptotic responses triggered by amputation. In planarians, amputation triggers a general proliferative response, which peaks at 6 hR, and a local response that peaks at 48 hR. Quantification of mitotic cells using an anti-phospho-histone 3 (PH3) antibody (Wenemoser and Reddien, 2010) revealed an increase in the mitotic response at both 6 hR and 48 hR in *bls2/3/5*(RNAi) versus control animals (Fig. 4A). The apoptotic response after amputation consists of two apoptotic peaks: one at 4 hR, which occurs close to the wound, and a second at 3 days of regeneration (dR), which is generalized (Pellettieri et al., 2010). Using a TUNEL assay (Fig. 4B) and by quantifying caspase 3 enzymatic activity (Fig. 4C), we demonstrated lower rates of apoptosis in *bls2/3/5*(RNAi) versus control planarians at both time points.

Distinct molecular and cellular responses are induced during healing of amputated tissue, notches (which imply tissue loss) and incisions (in which no tissue is removed). While control of cell proliferation and cell death is required in all scenarios, incision gives rise to just the first proliferative and apoptotic peaks. To examine how general the role of *bls2/3/5* is in attenuating cell proliferation and promoting cell death, we analyzed the response to notching and incision in *bls2/3/5*(RNAi) animals. In both situations, when compared with control RNAi, animals showed an increase in the number of mitotic cells (Fig. S4A,C) and a decrease in apoptosis (Fig. S4B,D), indicating that *bls2/3/5* attenuates proliferation and promotes cell death. These findings indicate that *Smed-bls2/3/5* attenuates cell proliferation and promotes cell death after any injury type, regardless of whether tissue is removed.

Cells are more numerous but smaller in starved *bls*(RNAi) planarians, resulting in no overall change in body size

The pattern of *bls2*, *bls3* and *bls5* expression in secretory cells in the prepharyngeal region and along the planarian margin suggests that these peptides may play a role in controlling cell proliferation and cell death, not only after injury but also during homeostasis, as planarians undergo continuous growth and degrowth according to nutrient availability. These changes in size are thought to be primarily due to modulation of cell number (Baguñá and Romero, 1981; Thommen et al., 2019) through regulation of the balance between proliferation and apoptosis (Pellettieri et al., 2010; González-Estévez et al., 2012a,b). In nutrient-poor environments planarians shrink by decreasing mitosis and increasing cell death. To determine whether *bls2/3/5* participates in regulating the proliferation/apoptosis equilibrium and body size during degrowth, we injected starved animals with *bls2/3/5* dsRNA for 3 weeks (Fig. 5A, Fig. S5A). The number of PH3$^+$ nuclei found in starved *bls2/3/5*RNAi animals versus control was only increased after the third week (Fig. 5B, Fig. S5C). Importantly, starved *bls2/3/5*(RNAi) planarians showed decreased apoptosis as the first week of inhibition compared with controls (Fig. 5C, Fig. S5D).

Development (2020) 147, dev184044. doi:10.1242/dev.184044

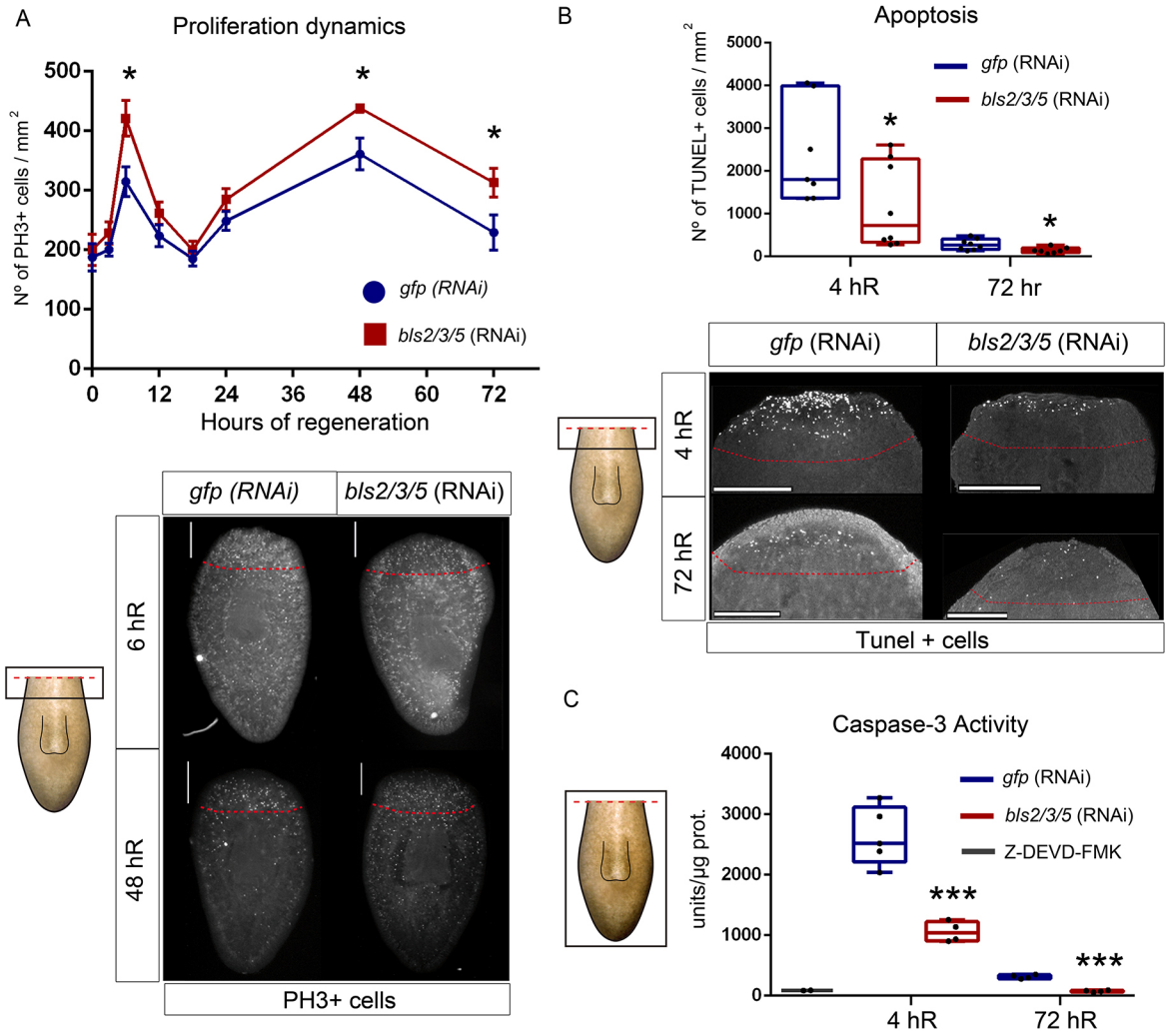

Fig. 4. After *bls2/3/5* RNAi, planarians exhibit increased proliferation and decreased apoptosis during anterior regeneration. (A) Quantification of PH3$^+$ cells at different stages of regeneration (controls, n>5; RNAi, n>5; *P<0.05). Lower panel shows anti-PH3 immunostaining of *gfp*(RNAi) and *bls2/3/5*(RNAi) animals. (B) Quantification of TUNEL$^+$ cells in *bls2/3/5*(RNAi) and control animals (controls, n>7; RNAi, n>7; *P<0.05). Lower panel shows TUNEL images. Images correspond to *z* projections. (C) Quantification of caspase 3 activity in *bls2/3/5*(RNAi) animals and controls (controls, n=4; RNAi, n=4; ***P<0.001). In the schematic drawings, the red dashed line represents the amputation plane and the square indicates the region analyzed. In the images, the red dashed line outlines the area quantified. Scale bars: 500 µm in A; 200 µm in B.

Although this alteration in the proliferation/apoptosis equilibrium did not give rise to larger animals (Fig. 5D), total cell number was higher in RNAi-injected animals versus controls (Fig. 5E). The fact that total cell number but not body size was increased in *bls2/3/5*(RNAi) animals implies a decrease in cell size. To examine changes in cell size, we focused our analysis on the epidermis, as epidermal cells form a monolayer that can be easily imaged in three dimensions. Nuclear staining revealed a higher density of epithelial cells in *bls2/3/5*(RNAi) animals (Fig. 5F, Fig. S5E), and quantification of mean epidermal cell area confirmed that this parameter was reduced in *bls2/3/5*(RNAi) animals when compared with controls (Fig. 5F′). A decrease in mean epidermal cell area could be due not to a reduction in the total cell volume but to narrowing of the cells in *bls2/3/5*(RNAi) animals. To quantify epidermal cell volume, we measured epidermal cell height (i.e. the mean distance from the apical to the basal margin of the cell) in animals immunostained with 6G10 antibody. We observed no differences in apical-basal distance in *bls2/3/5*(RNAi) animals with respect to controls (Fig. 5G,G′). Multiplication of mean cell area by mean cell height confirmed a decrease in epidermal cell volume in *bls2/3/5*(RNAi) animals versus controls (Fig. 5H,I). Changes in specific neural populations were evaluated by confocal imaging (Fig. 5J, Fig. S5F) and qPCR (Fig. S5G). The density of serotoninergic (*pitx*$^+$) (Currie and Pearson, 2013; März et al., 2013), octapaminergic (*tbh*$^+$) (Eisenhoffer et al., 2008) and dopaminergic (*th*$^+$) (Fraguas et al., 2011) neurons, and of chemoreceptors (*cintillo*$^+$) (Oviedo et al., 2003) was increased in *bls2/3/5*(RNAi) animals. Given the increase in cell density found in *bls2/3/5*(RNAi) animals after 3 weeks of inhibition, it could be that the increase in PH3$^+$ cells found at this time point results from the cell accumulation rather than from an effect of *bls2/3/5*(RNAi) on mitotic activity. This hypothesis is supported by the finding that the number of PH3$^+$ cells/area normalized by epidermal cell density of *bls2/3/5*(RNAi) is not significantly different from controls after 2 and 3 weeks of inhibition (Fig. S5H).

Importantly, continuous inhibition of *bls2/3/5*(RNAi) for 4 weeks resulted in the formation of overgrowths that were all located in the posterior part of the animal, mainly in the dorso-

Development (2020) 147, dev184044. doi:10.1242/dev.184044

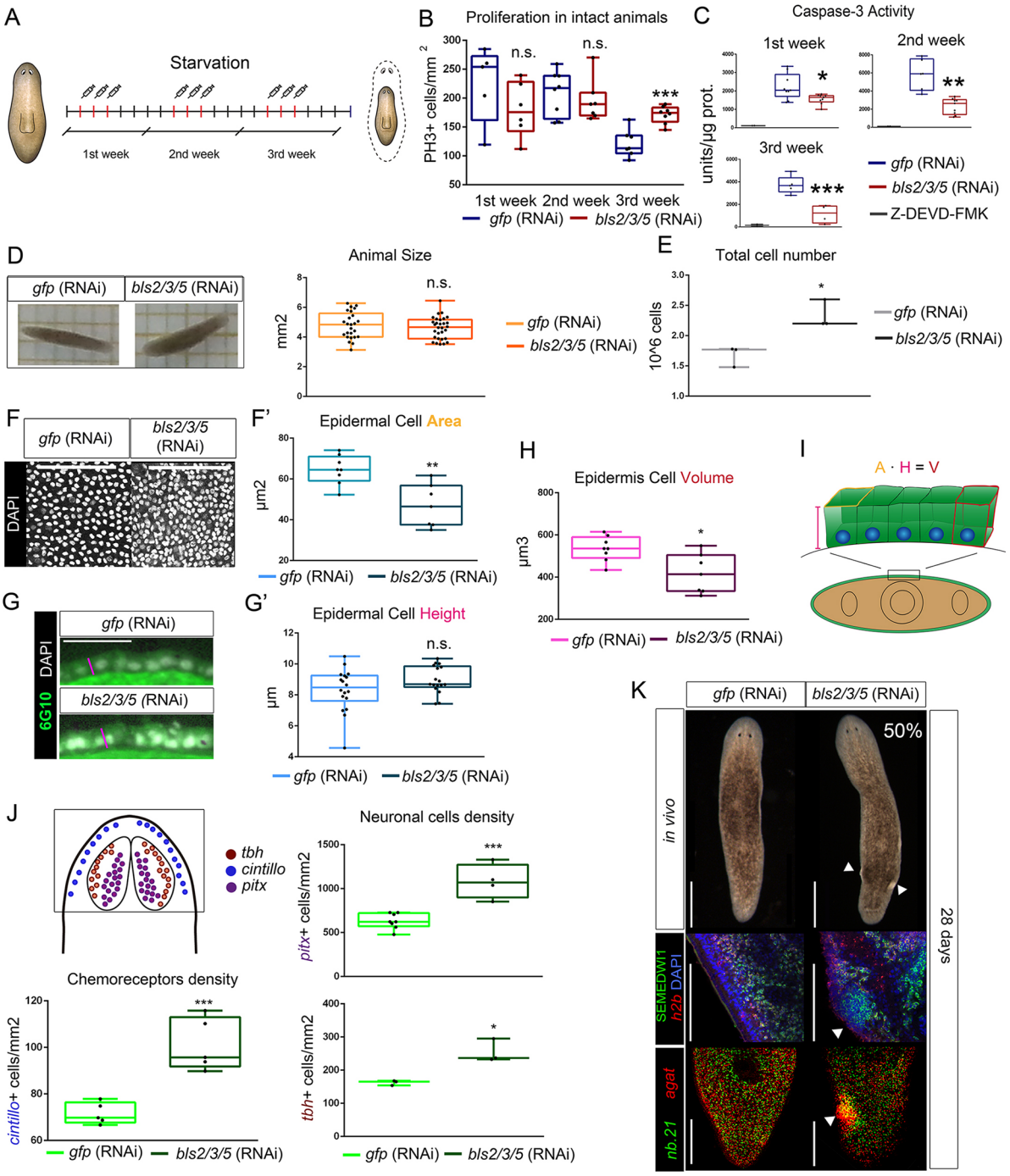

Fig. 5. In starving conditions, *bls2/3/5*(RNAi) animals show decreased cell death and cell accumulation but not an increase in body size. (A) Schematic depicting RNAi procedure. (B) Quantification of PH3$^+$ cells after 1 week of RNAi treatment (controls, *n*=5; RNAi, *n*=6; n.s.); 2 weeks of RNAi treatment (controls, *n*=7; RNAi, *n*=6; n.s.); and 3 weeks of RNAi treatment (controls, *n*=7; RNAi, *n*=9; ***P<0.001). Quantification is based in the number of PH3$^+$ cells per body area. (C) Quantification of caspase 3 after 1 week of RNAi treatment (controls, *n*=9; RNAi, *n*=9; *P<0.05); 2 weeks of treatment (controls, *n*=6; RNAi, *n*=9; **P<0.01); and 3 weeks of treatment (controls, *n*=10; RNAi, *n*=8; ***P<0.001). (D) Quantification of body area *in vivo* animals (controls, *n*=25; RNAi, *n*=30; n.s.). (E) Quantification of cell number (controls, *n*=3; RNAi, *n*=3; *P<0.05). Each biological replicate represents five animals. (F) DAPI staining of epithelial cells of the prepharyngeal region. (F′) Quantification of the mean epidermal cell area (A) (controls, *n*=8; RNAi, *n*=7; **P<0.01). (G) Transverse sections of planarian epidermis immunostained using anti-6G10. The distance from the basal to the apical part of the cells (epidermal cell height, H) is indicated with a pink line. (G′) Height quantification (controls, *n*=18, RNAi, *n*=17, n.s.). (H) Quantification of epidermal cell volume (V) (controls, *n*=8; RNAi, *n*=7; *P<0.05). (I) Schematic illustration of the measurements performed to quantify V. (J) Illustration depicts the expression of *cintillo*, *pitx* and *tbh*. The square indicates the area quantified. Quantification of *cintillo*$^+$ cells/head area (controls, *n*=5; RNAi, *n*=5; ***P<0.001), *pitx*$^+$ cells/head area (controls, *n*=8; RNAi, *n*=4; ***P<0.001), *tbh*$^+$ cells/head area (controls, *n*=3; RNAi, *n*=3; *P<0.05). (K) Half of the animals developed overgrowths after 4 weeks of *bls2/3/5* inhibition in starved conditions. Fluorescence *in situ* hybridization of *h2b* riboprobe combined with anti-SMEDWI-1 immunostaining, and fluorescence *in situ* hybridization with *agat*$^+$ and *nb.21* riboprobes (controls, *n*=60; RNAi, *n*=58). White arrowheads indicate overgrowths. Images from F and K correspond to *z* projections. Scale bars: 1 mm squares in D; 20 µm in F,G; 500 µm in K.

Development (2020) 147, dev184044. doi:10.1242/dev.184044

ventral margin (Fig. 5K). The molecular analysis of those overgrowths demonstrates the accumulation of postmitotic cells ($PIWI^+$ and $h2b^-$) (Solana et al., 2012), which express epidermal progenitor cell markers ($nb21^+$ and $agat1^+$) (Eisenhoffer et al., 2008) (Fig. 5K, Fig. S5I).

These data indicate that *bls2/3/5* promotes cell death during periods of shrinkage. *bls2/3/5* inhibition in starved planarians prevents the necessary reduction in cell number. Because cell size is reduced in *bls2/3/5*(RNAi) versus control animals, the increase in cell number observed in the former does not translate to larger body size. However, the accumulation of cells following long term inhibition does lead to overgrowths.

bls RNAi in fed planarians results in increases in cell number and body size

Planarians grow in size in nutrient-rich environments. This growth is due to an increase in cell number resulting from an increase in the mitosis:apoptosis ratio (Pellettieri et al., 2010; González-Estévez et al., 2012a,b). Our previous findings suggest that *bls2/3/5* inhibition in continuously fed planarians may lead to an increase in cell number and possibly also in body size. To test this hypothesis, planarians fed twice per week were injected with *bls2/3/5* dsRNA for 3 weeks (Fig. 6A, Fig. S6A,B). Compared with controls, these animals showed an increase in the rate of mitosis from the first week of inhibition (Fig. S6B,C), together with a decrease in the rate of apoptosis (Fig. 6C, Fig. S6E). Furthermore, during this 3-week period RNAi animals grew faster and reached a larger size (Fig. 6D) than controls (Fig. 6E). Quantification of dissociated cells revealed an increase in total cell number in *bls2/3/5*(RNAi) animals after 3 weeks of RNAi (Fig. 6F). In contrast to the results obtained for starved planarians, no differences in epidermal cell area or volume were observed in fed animals with respect to controls (Fig. 6G-J, Fig. S6F). Furthermore, quantification of neural and chemoreceptor cells revealed no differences in cell density between RNAi and control planarians (Fig. 6K, Fig. S6G).

These data indicate that *Smed-bls2/3/5* also promotes cell death and attenuates the rate of mitosis during growth periods, resulting in an increase in cell number. Remarkably, in fed animals this increase in cell number translates to an increase in body size, as cell size is maintained in this nutrient-rich context.

bls transcription depends on nutrient intake and mTOR signaling

Our results demonstrate that *bls2/3/5* subfamilies control the balance of cell proliferation and cell death in planarians not only after injury but also during normal homeostasis. We hypothesize that *bls2/3/5*-mediated signaling may constitute a general mechanism required to balance cell proliferation:cell death ratio in response to nutrient availability in planarians. According to our hypothesis, *bls2/3/5* activity would be required in nutrient-poor environments but not when food is readily available. As previously mentioned, planarian growth is sustained by increasing mitosis and decreasing cell death. After feeding, apoptosis remains very low and changes little (Fig. S7A), but proliferation increases and mitosis peaks at 3 h post-feeding (hpf) (Baguñá, 1974; Newmark and Sánchez Alvarado, 2000) (Fig. S7B). Thus, according to our hypothesis, *bls* expression should be actively downregulated a few hours after food ingestion to enable subsequent growth. Quantification of mRNA levels of *bls2*, *bls3* and *bls5* by qPCR at 3 hpf and 24 hpf revealed downregulation of all three *bls* mRNAs (Fig. 7A). This downregulation was also confirmed by FISH expression analysis: after feeding (24 hpf) expression of all three genes had decreased and/or the expression pattern had expanded and delocalized with respect to starved conditions (Fig. 7B, Fig. S7C,D).

To further understand the mechanism by which *bls2/3/5* balances cell proliferation:cell death ratio in response to nutrient intake, we analyzed its possible functional interaction with the mTOR pathway, a central regulator of cell metabolism (Saxton and Sabatini, 2017). In planarians, mTOR is upregulated in response to food intake, and its inhibition decreases proliferation and increases cell death, impeding growth (Peiris et al., 2012; Tu et al., 2012). Quantification of *bls2*, *bls3* and *bls5* expression levels in growing mTOR (RNAi) planarians shows a significant increase of *bls2*, *bls3* and *bls5* mRNA expression levels (Fig. 7C). Furthermore, quantification of mTOR expression levels in growing *bls2/3/5* (RNAi) animals shows upregulation of mTOR mRNA levels (Fig. 7D). Akt is a serine threonine protein kinase downstream of insulin and upstream of mTOR pathway (Yoon, 2017), inhibition of which in planarians increases cell death, decreases proliferation and impedes planarian growth (Peiris et al., 2016). qPCR quantification of *Akt* levels also demonstrates its upregulation in *bls2/3/5* RNAi planarians (Fig. 7D).

Overall, these suggest that expression of *bls2/3/5* subfamilies are constantly regulated in planarians to balance the cell proliferation: cell death ratio, being downregulated by nutrient intake to allow planarian growth. *bls2/3/5* is a novel gene that regulates cell number in response to nutrient intake, but it interacts with the evolutionary conserved insulin/Akt/mTOR metabolic network.

DISCUSSION

bls is a *de novo* gene family taxonomically restricted to the order Tricladida (planarians)

In this study, we have identified a new gene family, *blitzschnell* (*bls*), which appears to be an evolutionary novelty of Triclads (planarians), and is essential for the control of cell number in response to nutrient intake. In *S. mediterranea*, the *bls* family is composed of 15 members, grouped in five subfamilies (*bls1-bls5*). Members of *bls1* and *bls4* subfamilies are pseudogenes, while members of *bls2*, *bls3* and *bls5* subfamilies encode short peptides that contain a signal peptide (SP) and a coiled coil domain (CC). Fluorescent *in situ* hybridization analysis with specific riboprobes, demonstrates that *bls2*, *bls3* and *bls5* are all expressed in a subset of secretory cells, seeming tissue specific. Furthermore, we have only been able to find homologs of *bls* in species of the Tricladida order. Although the genomic databases of Platyhelminthes are incomplete, the *bls* family appears to be taxonomically restricted (Wilson et al., 2005). All described features: gene duplication and presence of pseudogenes (Tautz and Domazet-Lošo, 2011), short open reading frame with a signal peptide and a ISD (Neme and Tautz, 2013; Palmieri et al., 2014; Wilson et al., 2017; Werner et al., 2018), being expressed in specific cell types (Toll-Riera et al., 2009; Carvunis et al., 2012; Zhao et al., 2014), and being taxonomically restricted (Van Oss and Carvunis, 2019), are shared by genes that originated *de novo* during evolution. *De novo* genes, previously known as orphan genes (Schlötterer, 2015), could originate from an existing gene in the genome (Long et al., 2003), from non codifying genomic regions (Schlötterer, 2015) or from transposon domestication (McLysaght and Hurst, 2016). Although further phylogenetic studies are required to understand the origin of the *bls* family, our data favor the last two possibilities, as we could not find any homolog in species outside Tricladida, and we found transposable elements in the same genomic region where the *bls* family is found.

Development (2020) 147, dev184044. doi:10.1242/dev.184044

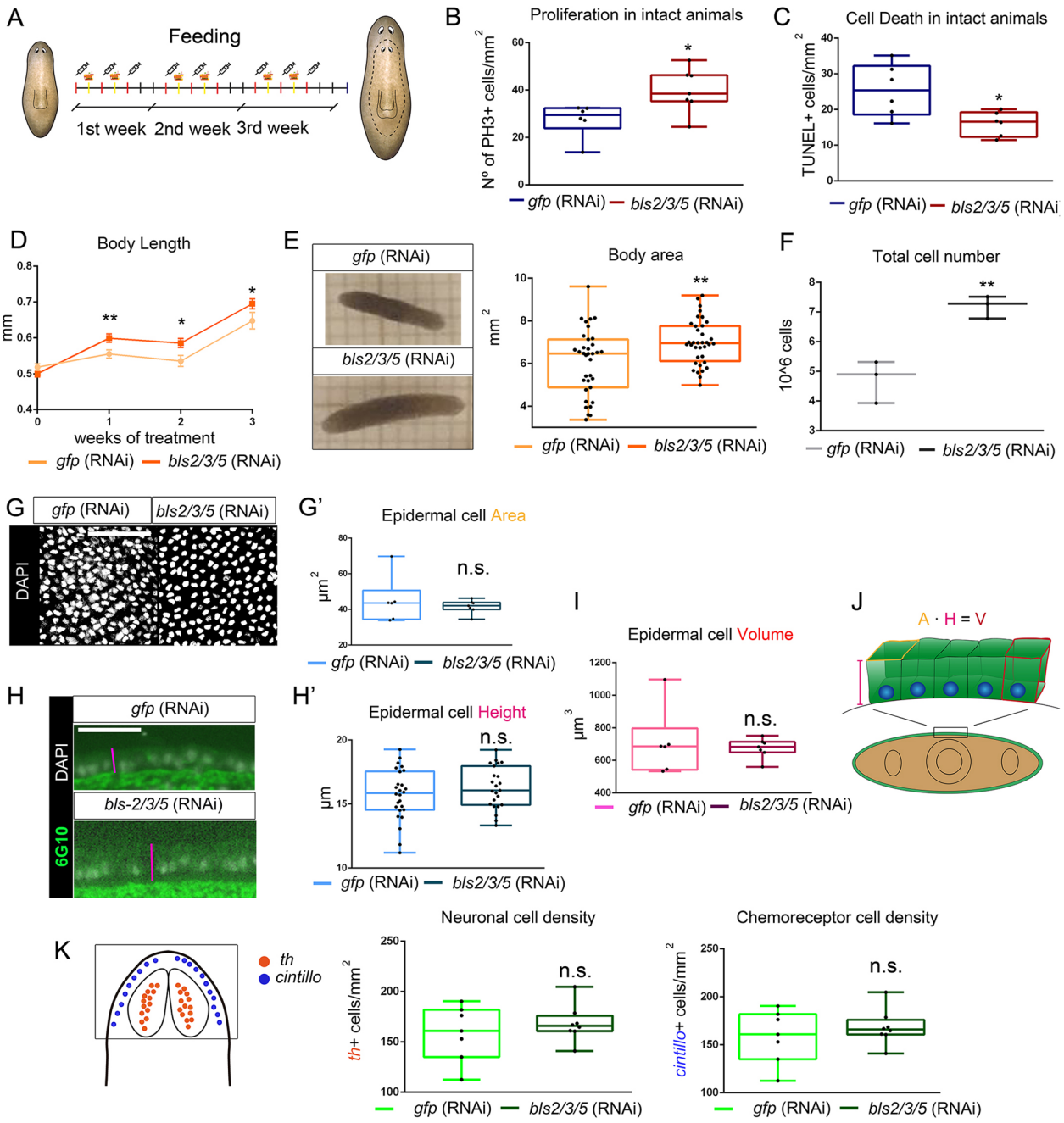

Fig. 6. In fed conditions, *bls2/3/5*(RNAi) animals show an increase in proliferation and a decrease in cell death, which results in larger animals. (A) Schematic depicting the RNAi procedure. (B) Quantification of PH3$^+$ cells after 3 weeks of RNAi treatment (controls, *n*=6; RNAi, *n*=7; **P*<0.05). Quantification is based in the number of PH3$^+$ cells per body area. (C) Quantification of TUNEL$^+$ cells after 3 weeks of RNAi treatment (controls, *n*=6; RNAi, *n*=6; **P*<0.05) (see Materials and Methods and Fig. S6E for details of quantification). (D) Length of control and RNAi animals (controls, *n* >35; RNAi, *n* >35; **P*<0.05, ***P*<0.01). (E) Quantification of body area in live animals (controls, *n*=35; RNAi, *n*=36; ***P*<0.01). (F) Quantification of cell number (controls, *n*=3; RNAi, *n*=3; ***P*<0.01). Each biological replicate represents five animals. (G) DAPI staining of epithelial cells of the prepharyngeal region. (G′) Quantification of mean epidermal cell area (A) (controls, *n*=6; RNAi, *n*=7; n.s.). (H) Transverse sections of planarian epidermis immunostained using anti-6G10. The distance from the basal to the apical part of the cell (epidermal cell height, H) is indicated with a pink line. (H′) Quantification of H (controls, *n*=26; RNAi, *n*=23; n.s.). (I) Quantification of epidermal cell volume (V) (controls, *n*=6; RNAi, *n*=7; n.s.). (J) Illustration showing measurements used to quantify V. (K) Quantification of *th*$^+$ cells/head area (controls, *n*=9; RNAi, *n*=6; n.s.) and *cintillo*$^+$ cells/head area (controls, *n*=7; RNAi, *n*=8; n.s.). Illustration depicts the expression of *th* and *cintillo*, and the square indicates the area quantified. Images from G′ correspond to *z* projections. Scale bars: 1 mm squares in D′; 20 µm in G,H.

The appearance of *bls* in Tricladida may be linked to the requirement for continuous and rapid modulation of cell number in response to nutrient availability

Our results demonstrate that *bls2/3/5* regulates the mitotis:apoptosis ratio in all scenarios analyzed. In homeostatic animals, the imbalance in this ratio led to an increase in cell number. Strikingly, this increase in cell number resulted in normal body size but smaller cell size in starved planarians, and in larger body size and normal cell size in fed animals (Fig. 8), suggesting an energy-dependent role for this gene. In other organisms, *de novo*

Development (2020) 147, dev184044. doi:10.1242/dev.184044

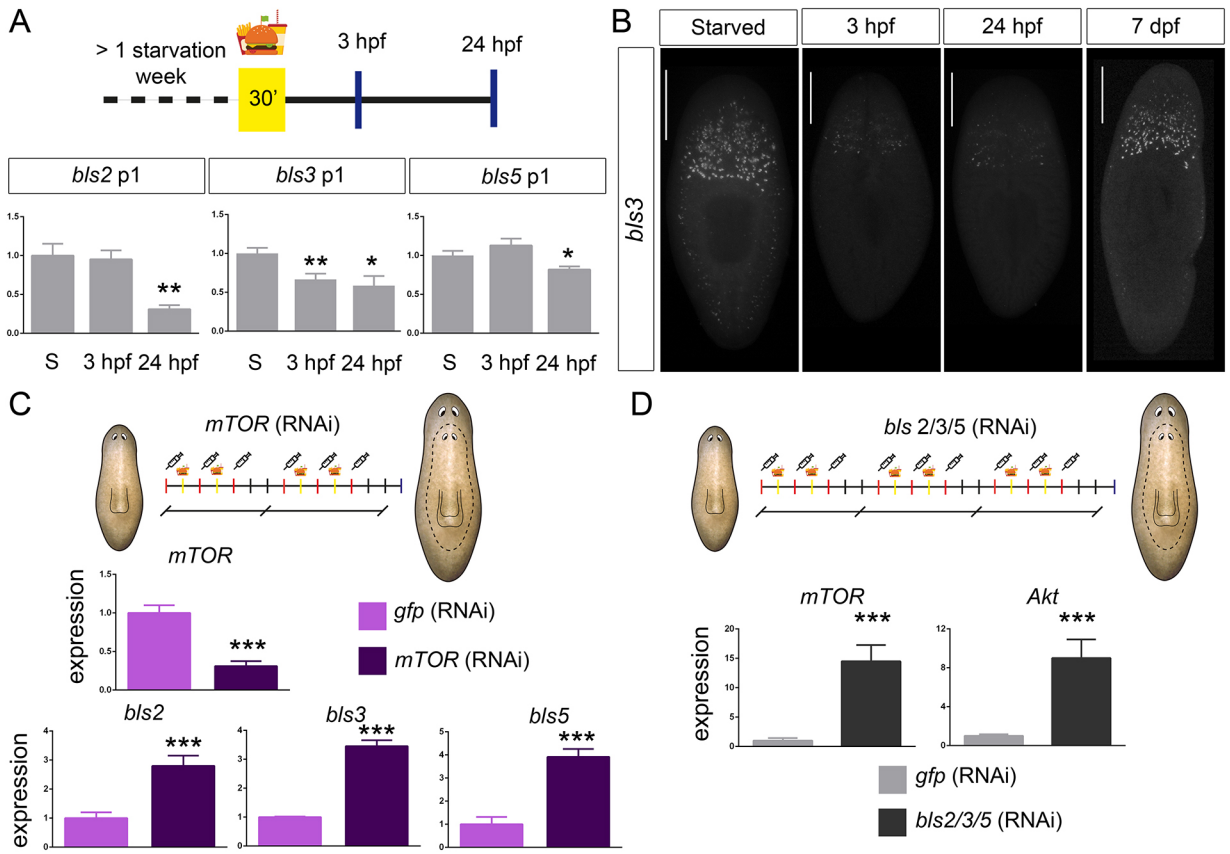

Fig. 7. *bls2*, *bls3* and *bls5* levels are regulated by food ingestion and by mTOR signaling. (A) Schematic depicting the experimental procedure. Animals were starved for more than 1 week and then fed for 30 min and fixed at different time points thereafter. Bar charts represent qRT-PCR quantification of *bls2*, *bls3* and *bls5* expression in starved animals (S) and in fed animals 3 and 24 h post-feeding (hpf). (B) Representative fluorescence *in situ* hybridization images of *bls3* before feeding and at different time points after feeding, demonstrating its reduced expression at 3 hpf and 24 hpf, and its recovery at 7 dpf. (C) qRT-PCR quantification of *bls2*, *bls3* and *bls5* expression in fed *mTOR* (RNAi) animals. Scheme depicts the RNAi procedure. (D) qRT-PCR quantification of *mTOR* and *Akt* expression in fed *bls2*/*3*/*5*(RNAi) animals. Scheme depicts the RNAi procedure. In all the panels, relative expression is plotted as $2^{-\Delta\Delta CT}$ values. Data are mean±s.d. **P*<0.05; ***P*<0.01, ****P*<0.001.

genes have been shown to play an important role in the response to biotic and/or abiotic stresses (Colbourne et al., 2011; Donoghue et al., 2011; Zhao et al., 2014). The observation that *bls2*, *bls3* and *bls5* are downregulated a few hours after food ingestion suggests that those genes can function as sensors of cell energy status. According to this hypothesis, *bls* expression is required to restrict cell number (and maintain cell size) in starvation conditions, but is downregulated after nutrient intake to allow for increases in cell number and body size (Fig. 8). The appearance of *bls* in Tricladida during evolution may be linked to the requirement for continuous modulation of cell number in response to nutrient availability in these organisms. The increase in the number of copies of *bls* family members and their tandem disposition suggest that they may be regulated by the same promoter, facilitating rapid regulation of their protein levels according to cell energy status.

Because *bls* genes share 70-100% of identity at the nucleotide level, we were unable to inhibit specific copies using RNAi, and were therefore unable to determine which gene copies perform the described function. For this reason, in this study we have ascribed this function to '*bls2/3/5*'. However, because all *bls* genes appear to follow the same expression dynamics and share almost identical amino acid sequences, we hypothesize that the gene copies encoding the SP and CC domains may perform the same function. This is in agreement with the aforementioned hypothesis of simultaneous regulation enabling rapid changes in expression. Nonetheless, we cannot rule out the possibility that copies that do not encode the CC domain may act as inhibitors.

bls genes could control the mitosis:apoptosis ratio and the cell size through interacting with the insulin/Akt/mTOR network

It has been described that *de novo* and TRG lack catalytic domains and normally interact with proteins in conserved networks (Arendsee et al., 2014). The presence of a SP suggests that *bls2*, *bls3* and *bls5* may be secreted and interact with components of those conserved pathways. Our results suggest that *bls2*/*3*/*5* may interact with members of the insulin/Akt/mTOR pathways, a universal mechanism that is activated by the extracellular nutrients and activates the signals required for growth. In planarians TORC-1 is downregulated during starvation and its inhibition decreases proliferation without affecting cell death. mTOR is upregulated in response to food intake in planarians, and its inhibition decreases proliferation and increases cell death, impeding growth (Peiris et al., 2012; Tu et al., 2012). mTOR hyper-activation, through PTEN or *smg-1* RNAi, promotes overproliferation and outgrowths (Oviedo et al., 2003; González-Estévez et al., 2012a,b). As *bls2*/*3*/*5* is expressed in nutrient-deprived conditions, it could be acting as an inhibitor of the insulin/Akt/mTOR network, which is in fact what our results suggest; mTOR and Akt are upregulated when *bls2*/*3*/*5* is inhibited, and vice versa.

Development (2020) 147, dev184044. doi:10.1242/dev.184044

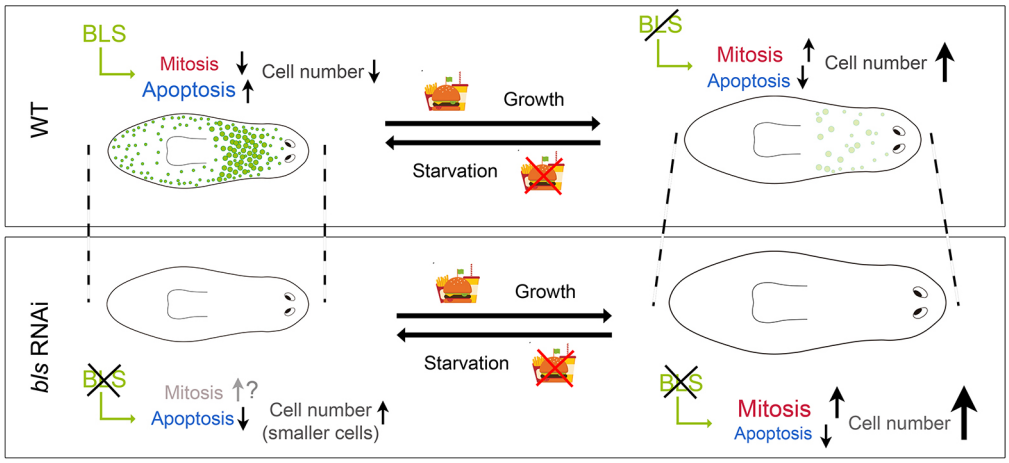

Fig. 8. Model representing *bls*-mediated control of cell number. In starving conditions *bls* is expressed and limits cell number and body size by promoting apoptosis without significantly affecting mitotic index. After feeding *bls* is downregulated, allowing an increase in mitotic cells and a decrease in cell death, which results in an increase in cell number. In starved *bls* RNAi animals, the mitosis:apoptosis ratio increases, as does total cell number. However, cells cannot maintain their size and body size does not increase. In fed *bls* RNAi animals, the mitosis:apoptosis ratio is even higher than in controls and cell number increases. This is accompanied by an increase in body size, as cells maintain their normal size.

An important result in this study is the finding that cellular responses are different according to the energetic status of the animals. *bls2/3/5* inhibition during starvation results in an early decrease in apoptosis and, with our methods, we could not detect an increase in mitotic index. In contrast, in growing animals both parameters seem to be affected. This could be also true when modulating the mTOR pathway, and the reason why different studies show opposite results regarding the mitotic rates mTOR silencing during homeostasis (Peiris et al., 2012; Tu et al., 2012). Cell death and proliferation analysis from specific nutritional context are required to understand the metabolic role of those signals.

Similarly, only fed animal cells are able to maintain the size after *bls2/3/5* inhibition. One possible explanation for the inability of starved animals to maintain cell size is that *bls2/3/5* silencing in these conditions may promote entry into M phase before cells reach their proper size. It is possible that, in wild-type planarians, cell cycle length varies according to nutritional status. Recent data suggest the existence of crosstalk between cell division and mitochondrial dynamics and metabolic pathways (Salazar-Roa and Malumbres, 2017). For example, yeast grown in nutrient-poor conditions adjust their cell-cycle duration to accommodate slower growth, so that the size at which cells divide is similar to that observed in nutrient-rich environments (Lloyd, 2013). It is possible that the duration of the cell cycle is longer in starved than fed animals, thereby ensuring that daughter cells reach the appropriate size. Promoting entry into M phase after *bls2/3/5* silencing could give rise to smaller cells in starved but not in fed animals. Because a mechanism through which mTOR signals regulate cell size is by controlling cell cycle (Fingar et al., 2002), and, as described above, planarian mTOR activity is regulated by food intake, interaction of *bls2/3/5* with this pathway could account for the smaller size of cells in starved animals. Analysis of the cell cycle in each of these different conditions will be required to test this hypothesis.

bls genes are tumor suppressors, inhibition of which favors regeneration

The appearance of overgrowths in starved *bls2/3/5* RNAi animals could be a consequence of the increase in cell density promoted after sustained inhibition cell death, as observed in tumoral processes (Lowe and Lin, 2000). *bls* genes as tumor suppressors during planarian degrowth. This observation presents us with a paradox: although caloric restriction extends lifespan (Pifferi and Aujard, 2019), in *bls2/3/5*(RNAi) planarians, food deprivation promotes hyperplasia and the formation of overgrowths, while fed *bls2/3/5*(RNAi) animals only increase body size with no apparent changes in patterning. A second key observation is that while *bls2/3/5* inhibition in starved animals promotes overgrowths, it favors regeneration after any kind of injury. This is consistent with the view that tumor suppressors evolved not to suppress tumor growth but to control cellular processes such as proliferation, cell death and cell differentiation, which are essential during embryogenesis and are activated during regeneration of complex tissues (Nacu and Tanaka, 2011). Perturbation of tumor suppressor function can enhance the regeneration of somatic stem cells in the hematopoietic system or endocrine cells (Pomerantz and Blau, 2013). Furthermore, inhibition of the Hippo pathway and consequent YAP/TAZ activation results in increases in organ size and promotes tumor formation in adult mice, but also promotes regeneration of the liver, gut, muscle and heart in mouse models (Moya and Halder, 2019).

Silencing of several known vertebrate tumor suppressors, including mTOR, p53 and Hippo, also induces the formation of overgrowths in planarians, but despite increasing proliferation does not promote proper regeneration. While TOR hyper-activation results in larger blastemas, these remain undifferentiated (González-Estévez et al., 2012a,b). Hippo hyper-activation also enhances the wound response and promotes expansion of the epidermal and muscle cell populations, and regeneration of larger structures such as the eyes (Lin and Pearson, 2017). However, this new tissue is not properly patterned (de Sousa et al., 2018). *bls* is the first family of genes described whose inhibition promotes faster but apparently normal regeneration. One possible explanation is that *bls* genes specifically control cell number (through regulation of the cell proliferation:cell death ratio) but not cell differentiation, as described for other signaling pathways such as Hippo (de Sousa et al., 2018). In this scenario, an increase in the number of cells during early stages of regeneration could accelerate the expression of wound-induced genes (Wenemoser et al., 2012), as we observed for *pitx*, and thereby promote more rapid appearance of regenerated structures.

Development (2020) 147, dev184044. doi:10.1242/dev.184044

Conclusions

In most animal species, the adult stage is distinguished from the embryonic stage by the maintenance of body size, cell number and proportions. However, long-lived animals, such as planarians, continuously regulate body size in adulthood by controlling cell number according to nutrient availability. Thus, the mechanisms described for other organisms, such as *Drosophila*, in which tissues 'know' their final size, may not apply to planarians (Nowak et al., 2013). Given that nutrient availability always fluctuates in nature, the *bls* family may represent an example of *de novo* genes that evolved in planarians to fulfil the requirement for continuous regulation of cell number according to nutrient availability. Other *de novo* genes have been implicated in increasing the fitness of the organism (Reinhardt et al., 2013; Schlötterer, 2015). Examples are described in cnidarians, in which *Hym301* regulates tentacle number (Khalturin et al., 2008), and in mollusks, in which each species expresses a unique set of secreted proteins that drives shell diversity (Aguilera et al., 2017). *De novo* genes are usually integrated into existing pathways, adding additional levels of regulation. *bls* genes may interact with members of the insulin/Akt/mTOR signaling pathways, which regulate growth in response to nutrient intake in planarians and in vertebrates. RNAi of components of these pathways does not fully phenocopy *bls2/3/5* RNAi. However, this signaling pathway should be thought of as a network in which each of these signals functions in a complex and dynamic manner, as opposed to a linear pathway. Future studies will need to determine whether the primary function of *bls* is to control proliferation or apoptosis, or both, and to elucidate the molecular integration of *bls* genes within the insulin/Akt/mTOR network. Given that the molecular signals controlling body and organ growth are also key players in most human cancers, understanding the mechanism by which *bls* genes act as tumor suppressors would help identify novel targets for the design of therapeutic strategies to modulate tissue growth.

MATERIALS AND METHODS

Planarian culture

The planarians used in this study are the asexual clonal strain of *S. mediterranea* BCN-10 biotype and were maintained as previously described (Fernandéz-Taboada et al., 2010) in planarian artificial medium (PAM) water (Cebrià and Newmark, 2005). Animals were fed twice per week with liver, and those used in starvation experiments were starved for 1 week.

RNAi screening

To identify genes involved in eye regeneration we performed a high density DNA microarray. We ran a gene expression profile of planarian tissues with control animals (control RNAi) and planarians without eyes (*Smed-sine oculis* RNAi) during early stages of head regeneration using the 'array star' software from Nymbelgene. Sixty-one candidate genes differentially expressed in those conditions were analyzed by RNAi (Eckelt, 2011). Among them we isolated *Smed-bls3*, which inhibition produced a faster eye regeneration.

Sequence and phylogenetic analyses

A fragment of *Smed-bls3* was identified from Eckelt (2011). Other members of the families were identified from the genome (Grohme et al., 2018) and amplified using specific primers (Table S3). The signal peptide was identified with SigalP v5.0 (Almagro Armenteros et al., 2019) and the coiled-coil domain was characterized using the tool available online from PRABI [Pole Rhone-Alpes de Bioinformatique; https://npsa-prabi.ibcp.fr/cgi-bin/npsa_automat.pl?page=npsa_lupas.html (Lupas et al., 1991)]. Sequence identity comparison was carried out using the pairwise alignment tool in Jalview suite v2.11 (Waterhouse et al., 2009).

To determine which members of each family were expressed, we mapped the RNAseq paired reads from adult wild-type animals (de Sousa et al., 2018) against assembly 2 of the *S. mediterranea* genome (Grohme et al., 2018) using *Bowtie2* (Langmead et al., 2009) v2.3.4, selecting the *-end-to-end* option. After alignment, we extracted the reads mapping the scaffolds of interest using *samtools view* (Li et al., 2009) v1.9. The final assessment was performed manually using the Integrative Genomics Viewer (Robinson et al., 2011) (IGV v2.4.4) to verify the families with mapped reads.

Sequence comparison against the GenBank database was performed using the NCBI BLAST network server (http://www.ncbi.nlm.nih.gov/Structure/cdd/wrpsb.cgi). Potential orthologs were searched for using tBLASTx where possible to allow a certain level of tolerance in case of a high degree of divergence. The search for orthologs was performed against transcriptomes and genomes from several Platyhelminthes species (Table S4) (Egger et al., 2015).

The IQ-tree web server (Trifinopoulos et al., 2016) was used to reconstruct the phylogenetic relationships between *Smed-bls* families. The nucleotide or protein sequences were first aligned using the alignment servers in JalView suite (MUSCLE for nucleotides and MAFFT for amino acids). Substitution model selection was performed automatically by the software, the number of bootstrap iterations was set to 1500 and default options were selected for the remaining parameters. The trees were visualized using FigTree v1.4.4 (http://tree.bio.ed.ac.uk/software/figtree/) with the default parameters.

Whole-mount *in situ* hybridization

Probes were synthesized *in vitro* using SP6 or T7 polymerase and DIG- or FITC- modified (Roche). RNA probes were purified by ethanol precipitation and the addition of 7.5 M ammonium acetate. For colorimetric whole-mount *in situ* hybridization, animals were sacrificed using 5% N-acetyl-L-cysteine (NAC), fixed with 4% formaldehyde and permeabilized with Reduction Solution (50 mM DTT, 1% NP-40, 0.5% SDS in 1× PBS). The fixative and whole-mount *in situ* hybridization protocol used has been previously described (Currie et al., 2016). For whole-mount fluorescent *in situ* hybridization, animals were sacrificed with 7.5% NAC and fixed with 4% formaldehyde. Fluorescent in situ hybridization was carried out as described previously (King and Newmark, 2013). For double fluorescent *in situ* hybridization (dFISH) an azide step (150 mM sodium azide for 45 min at room temperature) was added. Nuclei were stained with DAPI (1:5000; Sigma). For fluorescent *in situ* hybridization of paraffin sections, animals were sacrificed with 2% HCl and fixed with 4% PFA. Paraffin embedding and sectioning were carried out as previously described (Cardona et al., 2005),slides were de-waxed and re-hydrated, and antigen retrieval step was performed as previously described (Sureda-Gómez et al., 2016). Sections were hybridized with the corresponding probes for 16 h and incubated with antibody diluted 1% BSA for 16 h. Both steps were carried out in a humidified chamber (Cardona et al., 2005).

Immunohistochemistry

Whole-mount immunohistochemistry was performed as previously described (Ross et al., 2015). Animals were killed with 2% HCl and fixed with 4% formaldehyde. The following antibodies used in these experiments: mouse anti-synapsin (anti-SYNORF1, 1:50; Developmental Studies Hybridoma Bank), mouse anti-VC1 (anti-arrestin, 1:15,000, kindly provided by Professor Hidefumi Orii, University of Hyogo, Kobe, Japan), rabbit anti-phospho-histone H3 (Ser10) (D2C8) (PH3) (1:500; Cell Signaling Technology; 9701) and anti-SMEDWI-1 antibody (1:1000, kindly provided by Professor Kerstin Bartscherer, Hubrecht Institute, Utrecht, The Netherlands). The secondary antibodies used were Alexa 488-conjugated goat anti-mouse (1:400; Molecular Probes; A28175) and Alexa 568-conjugated goat anti-rabbit (1:1000; Molecular Probes; A-11011). Nuclei were stained with DAPI (1:5000). For immunohistochemistry of paraffin sections, animals were killed and treated as described above. Sections were blocked in 1% bovine serum albumin (BSA) in 1×PBS for 1 h at room temperature and then incubated with primary antibodies diluted in blocking solution (mouse anti-muscle fiber antibody, 6G10, 1:400; Developmental Studies Hybridoma Bank) for 16 h at 4°C in a humidified chamber. Subsequently, sections were washed in 1×PBS and incubated with secondary antibodies (anti-mouse Alexa 488-conjugated antibody, 1:400; Molecular Probes; A28175) in blocking solution for 3 h at room temperature in a humidified chamber. Nuclei were stained with DAPI (1:5000; Sigma-Aldrich).

Development (2020) 147, dev184044. doi:10.1242/dev.184044

TUNEL assay

For the whole-mount TUNEL assay, animals were sacrificed with 10% NAC, fixed with 4% FA and permeabilized with 1% sodium dodecyl sulfate (SDS) solution. A TUNEL assay was carried out as described previously (Pellettieri et al., 2010) using the ApopTag Red *In situ* Apoptosis Detection Kit (CHEMICON, S7165). Nuclei were stained with DAPI (1:5000; Sigma-Aldrich). For TUNEL assay on paraffin sections, animals were killed and treated as described above. Sections were treated as described previously (Pellettieri et al., 2010) and after the dewaxing step a proteinase K step was added for permeabilization. Next, we used the ApopTag Red *In situ* Apoptosis Detection Kit (CHEMICON, S7165). Positive cells were counted in at least 9 representative sagittal sections per animal, and the overall mean value was determined. Six animals were analyzed per condition.

RNA interference analysis

Double-strand RNA (dsRNA) was synthesized by *in vitro* transcription (Roche) as previously described (Sanchez Alvarado and Newmark, 1999). dsRNA (3×32.2 nl) was injected into the digestive system of each animal on three consecutive days (1 round). The experiments in which regeneration was studied consisted of two consecutive rounds of injections and an amputation at the end of each round. In experiments in which planarians were starved, animals underwent three or four consecutive rounds of injection, without amputation. In experiments involving fed animals, planarians received dsRNA injections on three non-consecutive days per week and were fed on the two intervening days. This process was repeated for 3 weeks in total. All control animals were injected with dsRNA of green fluorescent protein (GFP). RNAi of subfamilies *bls2*, *bls3* and *bls5* was carried out using two different RNA sequences, both of which produced the same phenotype when injected in regenerating planarians (Table S3, Table S8). The sequences corresponded to the full *bls3* sequence and to a smaller region showing the greatest similarity between the *bls2*, *bls3* and *bls5* subfamilies. In the case of the second RNA sequence, inhibition of all members of the transcribed families was demonstrated by qPCR analysis (Figs S3B,C, S5B, S6B)

Feeding experiments

In long-term growth experiments involving RNAi, animals were fed twice per week: food was provided in the morning and removed at the end of the day (Fig. 5A, Fig. S5A). PAM water was replenished three times per week. To study gene expression after feeding, we analyzed planarians that had been starved for 1 week and then fed for 30 min. Next, we removed the food and replenished the PAM water (Fig. 7A). Hours post feeding (hpf) were counted from the moment of removal of the last piece of food.

Quantitative real-time PCR

Total RNA was extracted from a pool of five planarians per condition using TRIzol reagent (Invitrogen). cDNA was synthesized as previously described (Almuedo-Castillo et al., 2014). Expression levels were normalized to that of the housekeeping gene *ura4*. All experiments were performed using three biological and three technical replicates for each condition. The design of specific primers corresponding to the 5′ region for subfamilies *bls2*, *bls3* and *bls5* allowed verification of the inhibition of the three gene families after RNAi. All primers used in this study are shown in Table S3.

Caspase 3 activity assay

For each condition, protein extraction was performed in five planarians. The protein concentration of the cell lysates was measured using Bio-Rad protein reagent. Fluorometric analysis of caspase 3 activity was performed as described previously (González-Estévez et al., 2007) using 20 mg of protein extract, which was incubated for 2 h at 37°C with 20 µM caspase 3 substrate Ac-DEVD-AMC or 2 ml from a stock of 1 mg/ml for a final volume of 150 µl. Using a Fluostar Optima microplate fluorescence reader (BMG Labtech), fluorescence was measured in a luminescence spectrophotometer (Perkin- Elmer LS-50), applying the following settings: excitation, 380 nm; emission, 440 nm. Three technical replicates were analyzed per condition.

Cell number and cell volume analyses

To quantify total cell number, planarian cells were dissociated with trypsin and the nuclei stained with DAPI (Moritz et al., 2012). The cell suspension was transferred to a Neubauer chamber, cells were manually counted on three occasions, and the mean value calculated. Five planarians were analyzed per biological replicate, and three replicates were analyzed per condition. Mean cell volume (V) was calculated by multiplying mean epidermal cell area (A) by epidermal cell height (H). To quantify the mean epidermal cell area, the prepharyngeal epidermal area was imaged and the number of nuclei per area was quantified. To determine mean epidermal cell height, the distance between the apical to the basal part of the cell was measured. Measurements were taken in three different regions of the same section and the mean value obtained.

Imaging and quantification

Whole-mount and fluorescent *in situ* hybridization, and immunohistochemistry images were captured with a ProgRes C3 camera from Jenoptik (Jena). A Leica MZ16F microscope (Leica Microsystems) was used to observe the samples and obtain fluorescent *in situ* hybridization, immunostaining and TUNEL images. A Leica TCS SPE confocal microscope (Leica Microsystems) was used to obtain confocal images of whole-mount fluorescent *in situ* hybridization, immunostaining and TUNEL assays. Representative confocal stacks for each experimental condition are shown. Cell counting of $PH3^+$, $TUNEL^+$ and specific cell types was carried out by eye quantification in a previous defined area of each animal. Areas are schematically indicated in each figure. The total number of positive cells was divided by these areas. Images were blind analyzed and later grouped according to each genotype. To calculate the ratio of $PH3^+$cells:epidermal cell density, the number of $PH3^+$ cells/mm^2 counted per animal was divided by the epidermal cell density quantified in a predetermined prepharyngeal region.

Statistical analyses

Statistical analyses were performed using GraphPad Prism 6. Two-sided Student's *t*-tests (α=0.05) were performed to compare the means of two populations. Two-sided Fisher's exact tests were used to compare two phenotypic variants between two populations. Fisher.test from the R package was used to compare more than two phenotypic variants between two populations.

Statistical data presentation

Results were plotted using GraphPad Prism 6. To compare two populations, we used box plots depicting the median, the 25th and 75th percentiles (box), and all included data points (black dots). Whiskers extend to the largest data point within the 1.5 interquartile range of the upper quartile and to the smallest data point within the 1.5 interquartile lower range of the quartile. To plot data points over time, we used *xy* plots, in which each dot represents the mean and bars represent the standard error. Each dot is connected with the next in an arbitrary manner. To visualize the percentage phenotype in each population we used the Stacked Bars plot in R. Each phenotype is assigned a distinct color.

Acknowledgements

We thank all members of the Emili Saló, Teresa Adell and Francesc Cebrià labs for their suggestions and discussion of the results; Patrik Aloy for tertiary structure prediction of the peptide; Owen Howard for English language editing assistance; and the anonymous reviewers for their useful comments.

Competing interests

The authors declare no competing or financial interests.

Author contributions

Conceptualization: E.P.-C., E.S., T.A.; Methodology: E.P.-C., E.S., T.A.; Formal analysis: E.P.-C., T.A.; Investigation: E.P.-C., M.M.-B., C.H.-Ú, D.F.-M., K.E., N.d.S.; Data curation: E.P.-C.; Writing - original draft: E.P.-C., T.A.; Writing - review & editing: E.P.-C., T.A.; Supervision: E.S., T.A.; Project administration: J.G.-F., E.S., T.A.; Funding acquisition: J.G.-F., E.S., T.A.

Funding

E.P.-C. is the recipient of a Formación del Profesorado Investigador scholarship from the Spanish Ministerio de Ciencia, Innovación y Universidades. E.S. and T.A. received funding from the Ministerio de Educación y Ciencia (BFU2017-83755-P and BFU2014-56055-P). E.S. and T.A. benefit from funding from Agencia de Gestió d'Ajuts Universitaris i de Recerca (Genereliat de Catalunya) (2017SGR-1455).

E.S. received funding from Agencia de Gestió d'Ajuts Universitaris i de Recerca (Genereliat de Catalunya) (2009SGR1018). The funders have no role in the study design, data collection and analysis, decision to publish, or manuscript preparation.

Data availability

Nucleotide sequence data reported are available in the Third Party Annotation Section of the DDBJ/ENA/GenBank databases under the accession numbers TPA: BK010973-BK010987. GenBank accession numbers of *bls* sequences are as follows: *bls1a* (BK010973), *bls1b* (BK010974), *bls2a* (BK010975), *bls2b* (BK010976), *bls3a* (BK010977), *bls3b* (BK010978), *bls3c* (BK010979), *bls3d* (BK010980), *bls3e* (BK010981), *bls3f* (BK010982), *bls3g* (BK010983), *bls4a* (BK010984), *bls4b* (BK010985), *bls5a* (BK010986) and *bls5b* (BK010987).

Supplementary information

Supplementary information available online at http://dev.biologists.org/lookup/doi/10.1242/dev.184044.supplemental

Peer review history

The peer review history is available online at https://dev.biologists.org/lookup/doi/10.1242/dev.184044.reviewer-comments.pdf

References

Aguilera, F., McDougall, C. and Degnan, B. M. (2017). Co-option and de novo gene evolution underlie molluscan shell diversity. *Mol. Biol. Evol.* **34**, 779-792. doi: 10.1093/molbev/msw294

Almagro Armenteros, J. J., Tsirigos, K. D., Sønderby, C. K., Petersen, T. N., Winther, O., Brunak, S., Von Heijne, G. and Nielsen, H. (2019). SignalP 5.0 improves signal peptide predictions using deep neural networks. *Nat. Biotechnol.* **37**, 420-423. doi:10.1038/s41587-019-0036-z

Almuedo-Castillo, M., Crespo, X., Seebeck, F., Bartscherer, K., Salò, E. and Adell, T. (2014). JNK controls the onset of mitosis in planarian stem cells and triggers apoptotic cell death required for regeneration and remodeling. *PLoS Genet.* **10**, e1004400. doi:10.1371/journal.pgen.1004400

Arendsee, Z. W., Li, L. and Wurtele, E. S. (2014). Coming of age: orphan genes in plants. *Trends Plant Sci.* **19**, 698-708. doi:10.1016/j.tplants.2014.07.003

Baguñá, J. (1974). Dramatic mitotic response in planarians after feeding, and a hypothesis for the control mechanism. *J. Exp. Zool.* **190**, 117-122. doi:10.1002/jez.1401900111

Baguñá, J. (1976). Mitosis in the intact and regenerating planarian Dugesia mediterranea n.sp. I. Mitotic studies during growth, feeding and starvation. *J. Exp. Zool.* **195**, 53-64. doi:10.1002/jez.1401950106

Baguñá, J. and Salo, E. (1984). Regeneration and pattern formation in planarians I. The pattern of mitosis in anterior and posterior regeneration in Dugesia (G) tigrina, and a new proposal for blastema formation. *Development* **83**, 63-80.

Baguñá, J. and Romero, R. (1981). Quantitative analysis of cell types during growth, degrowth and regeneration in the planarians Dugesia mediterranea and Dugesia tigrina. *Hydrobiologia* **84**, 181-194. doi:10.1007/BF00026179

Cardona, A., Fernández, J., Solana, J. and Romero, R. (2005). An in situ hybridization protocol for planarian embryos: monitoring myosin heavy chain gene expression. *Dev. Genes Evol.* **215**, 482-488. doi:10.1007/s00427-005-0003-1

Carvunis, A.-R., Rolland, T., Wapinski, I., Calderwood, M. A., Yildirim, M. A., Simonis, N., Charloteaux, B., Hidalgo, C. A., Barbette, J., Santhanam, B. et al. (2012). Proto-genes and de novo gene birth. *Nature* **487**, 370-374. doi:10.1038/nature11184

Cebrià, F., Nakazawa, M., Mineta, K., Ikeo, K., Gojobori, T. and Agata, K. (2002). Dissecting planarian central nervous system regeneration by the expression of neural-specific genes. *Dev. Growth Differ.* **44**, 135-146. doi:10.1046/j.1440-169x.2002.00629.x

Cebrià, F. and Newmark, P. A. (2005). Planarian homologs of netrin and netrin receptor are required for proper regeneration of the central nervous system and the maintenance of nervous system architecture. *Development* **132**, 3691-3703. doi:10.1242/dev.01941

Colbourne, J. K., Pfrender, M. E., Gilbert, D., Thomas, W. K., Tucker, A., Oakley, T. H., Tokishita, S., Aerts, A., Arnold, G. J., Basu, M. K. et al. (2011). The ecoresponsive genome of daphnia pulex. *Science* **331**, 555-561. doi:10.1126/science.1197761

Currie, K. W. and Pearson, B. J. (2013). Transcription factors lhx1/5-1 and pitx are required for the maintenance and regeneration of serotonergic neurons in planarians. *Development* **140**, 3577-3588. doi:10.1242/dev.098590

Currie, K. W., Brown, D. D. R., Zhu, S., Xu, C. J., Voisin, V., Bader, G. D. and Pearson, B. J. (2016). HOX gene complement and expression in the planarian Schmidtea mediterranea. *EvoDevo* **7**, 7. doi:10.1186/s13227-016-0044-8

de Sousa, N., Rodríguez-Esteban, G., Rojo-Laguna, J. I., Saló, E. and Adell, T. (2018). Hippo signaling controls cell cycle and restricts cell plasticity in planarians. *PLoS Biol.* **16**, e2002399. doi:10.1371/journal.pbio.2002399

Dhanasekaran, D. N. and Reddy, E. P. (2017). JNK-signaling: a multiplexing hub in programmed cell death. *Genes Cancer* **8**, 682-694. doi: 10.18632/genesandcancer.155

Donoghue, M. T., Keshavaiah, C., Swamidatta, S. H. and Spillane, C. (2011). Evolutionary origins of Brassicaceae specific genes in Arabidopsis thaliana. *BMC Evol. Biol.* **11**, 47. doi:10.1186/1471-2148-11-47

Eckelt, K. (2011). *Multi-Approach Analysis for Identification and Functional Characterization of Eye Regeneration Related Genes of Schmidtea Mediterranea*. Barcelona, Spain: University of Barcelona.

Egger, B., Lapraz, F., Tomiczek, B., Müller, S., Dessimoz, C., Girstmair, J., Škunca, N., Rawlinson, K., Cameron, C., Beli, E. et al. (2015). A transcriptomic-phylogenomic analysis of the evolutionary relationships of flatworms. *Curr. Biol.* **25**, 1347-1353. doi:10.1016/j.cub.2015.03.034

Eisenhoffer, G. T., Kang, H. and Alvarado, A. S. (2008). Molecular analysis of stem cells and their descendants during cell turnover and regeneration in the planarian schmidtea mediterranea. *Cell Stem Cell* **3**, 327-339. doi:10.1016/j.stem.2008.07.002

Fernandéz-Taboada, E., Moritz, S., Zeuschner, D., Stehling, M., Scholer, H. R., Salo, E. and Gentile, L. (2010). Smed-SmB, a member of the LSm protein superfamily, is essential for chromatoid body organization and planarian stem cell proliferation. *Development* **137**, 1055-1065. doi:10.1242/dev.042564

Fincher, C. T., Wurtzel, O., de Hoog, T., Kravarik, K. M. and Reddien, P. W. (2018). Cell type transcriptome atlas for the planarian Schmidtea mediterranea. *Science* **360**, eaaq1736. doi:10.1126/science.aaq1736

Fingar, D. C., Salama, S., Tsou, C., Harlow, E. and Blenis, J. (2002). Mammalian cell size is controlled by mTOR and its downstream targets S6K1 and 4EBP1/eIF4E. *Genes Dev.* **16**, 1472-1487. doi:10.1101/gad.995802

Fraguas, S., Barberán, S. and Cebrià, F. (2011). EGFR signaling regulates cell proliferation, differentiation and morphogenesis during planarian regeneration and homeostasis. *Dev. Biol.* **354**, 87-101. doi:10.1016/j.ydbio.2011.03.023

Gokhale, R. H. and Shingleton, A. W. (2015). Size control: the developmental physiology of body and organ size regulation. *Wiley Interdiscip. Rev. Dev. Biol.* **4**, 335-356. doi:10.1002/wdev.181

González, A. and Hall, M. N. (2017). Nutrient sensing and TOR signaling in yeast and mammals. *EMBO J.* **36**, 397-408. doi:10.15252/embj.201696010

González-Estévez, C., Felix, D. A., Aboobaker, A. A. and Salo, E. (2007). Gtdap-1 promotes autophagy and is required for planarian remodeling during regeneration and starvation. *Proc. Natl. Acad. Sci. USA* **104**, 13373-13378. doi:10.1073/pnas.0703588104

González-Estévez, C., Felix, D. A., Rodríguez-Esteban, G. and Aboobaker, A. A. (2012a). Decreased neoblast progeny and increased cell death during starvation-induced planarian degrowth. *Int. J. Dev. Biol.* **56**, 83-91. doi:10.1387/ijdb.113452cg

González-Estévez, C., Felix, D. A., Smith, M. D., Paps, J., Morley, S. J., James, V., Sharp, T. V. and Aboobaker, A. A. (2012b). SMG-1 and mTORC1 act antagonistically to regulate response to injury and growth in planarians. *PLoS Genet.* **8**, e1002619. doi:10.1371/journal.pgen.1002619

Grohme, M. A., Schloissnig, S., Rozanski, A., Pippel, M., Young, G. R., Winkler, S., Brandl, H., Henry, I., Dahl, A., Powell, S., et al. (2018). The genome of Schmidtea mediterranea highlights the plasticity of cellular core mechanisms. *Nature* **554**, 56-61. doi: 10.1038/nature2547

Guertin, D. A. and Sabatini, D. M. (2006). Cell size control. *eLS* 1-10. doi:10.1038/npg.els.0003359

Hariharan, I. K. (2015). Organ size control: lessons from Drosophila. *Dev. Cell* **34**, 255-265. doi:10.1016/j.devcel.2015.07.012

Khalturin, K., Anton-Erxleben, F., Sassmann, S., Wittlieb, J., Hemmrich, G. and Bosch, T. C. G. (2008). A novel gene family controls species-specific morphological traits in Hydra. *PLoS Biol.* **6**, 2436-2449. doi:10.1371/journal.pbio.0060278

King, R. S. and Newmark, P. A. (2013). In situ hybridization protocol for enhanced detection of gene expression in the planarian Schmidtea mediterranea. *BMC Dev. Biol.* **13**, 8. doi:10.1186/1471-213X-13-8

Langmead, B., Trapnell, C., Pop, M. and Salzberg, S. L. (2009). Ultrafast and memory-efficient alignment of short DNA sequences to the human genome. *Genome Biol.* **10**, R25. doi:10.1186/gb-2009-10-3-r25

Li, H., Handsaker, B., Wysoker, A., Fennell, T., Ruan, J., Homer, N., Marth, G., Abecasis, G. and Durbin, R. (2009). The sequence alignment/map format and SAMtools. *Bioinformatics* **25**, 2078-2079. doi:10.1093/bioinformatics/btp352

Lin, A. Y. T. and Pearson, B. J. (2017). Yorkie is required to restrict the injury responses in planarians. *PLoS Genet.* **13**, e1006874. doi:10.1371/journal.pgen.1006874

Lloyd, A. C. (2013). The regulation of cell size. *Cell* **154**, 1194-1205. doi:10.1016/j.cell.2013.08.053

Long, M., Betrán, E., Thornton, K. and Wang, W. (2003). The origin of new genes: glimpses from the young and old. *Nat. Rev. Genet.* **4**, 865-875. doi:10.1038/nrg1204

Lowe, S. W. and Lin, A. W. (2000). Apoptosis in cancer. *Carcinogenesis* **21**, 485-495. doi:10.1093/carcin/21.3.485

Lupas, A., Van Dyke, M. and Stock, J. (1991). Predicting coiled coils from protein sequences. *Science* **252**, 1162-1164. doi:10.1126/science.252.5009.1162

März, M., Seebeck, F. and Bartscherer, K. (2013). A Pitx transcription factor controls the establishment and maintenance of the serotonergic lineage in planarians. *Development* **140**, 4499-4509. doi:10.1242/dev.100081
Mclysaght, A. and Hurst, L. D. (2016). Open questions in the study of de novo genes: what, how and why. *Nat. Rev. Genet.* **17**, 567-578. doi:10.1038/nrg.2016.78
Miller, C. M. and Newmark, P. A. (2012). An insulin-like peptide regulates size and adult stem cells in planarians. *Int. J. Dev. Biol.* **56**, 75-82. doi:10.1387/ijdb.113443cm
Miyaoka, Y., Ebato, K., Kato, H., Arakawa, S., Shimizu, S. and Miyajima, A. (2012). Hypertrophy and unconventional cell division of hepatocytes underlie liver regeneration. *Curr. Biol.* **22**, 1166-1175. doi:10.1016/j.cub.2012.05.016
Molina, M. D., Neto, A., Maeso, I., Gómez-Skarmeta, J. L., Saló, E. and Cebrià, F. (2011). Noggin and noggin-like genes control dorsoventral axis regeneration in planarians. *Curr. Biol.* **21**, 300-305. doi:10.1016/j.cub.2011.01.016
Moritz, S., Stöckle, F., Ortmeier, C., Schmitz, H., Rodíguez-Esteban, G., Key, G. and Gentile, L. (2012). Heterogeneity of planarian stem cells in the S/G2/M phase. *Int. J. Dev. Biol.* **56**, 117-125. doi:10.1387/ijdb.113440sm
Moya, I. M. and Halder, G. (2019). Hippo–YAP/TAZ signalling in organ regeneration and regenerative medicine. *Nat. Rev. Mol. Cell Biol.* **20**, 211-226. doi:10.1038/s41580-018-0086-y
Nacu, E. and Tanaka, E. M. (2011). Limb regeneration: a new development? *Annu. Rev. Cell Dev. Biol.* **27**, 409-440. doi:10.1146/annurev-cellbio-092910-154115
Neme, R. and Tautz, D. (2013). Phylogenetic patterns of emergence of new genes support a model of frequent de novo evolution. *BMC Genomics* **14**, 117. doi:10.1186/1471-2164-14-117
Newmark, P. A. and Sánchez Alvarado, A. (2000). Bromodeoxyuridine specifically labels the regenerative stem cells of planarians. *Dev. Biol.* **220**, 142-153. doi:10.1006/dbio.2000.9645
Nowak, K., Seisenbacher, G., Hafen, E. and Stocker, H. (2013). Nutrient restriction enhances the proliferative potential of cells lacking the tumor suppressor PTEN in mitotic tissues. *eLife* **2013**, 1-21. doi:10.7554/eLife.00380.044
Oviedo, N. J., Newmark, P. A. and Sánchez Alvarado, A. (2003). Allometric scaling and proportion regulation in the freshwater planarian Schmidtea mediterranea. *Dev. Dyn.* **226**, 326-333. doi:10.1002/dvdy.10228
Oviedo, N. J., Pearson, B. J., Levin, M. and Sanchez Alvarado, A. (2008). Planarian PTEN homologs regulate stem cells and regeneration through TOR signaling. *Dis. Model. Mech.* **1**, 131-143. doi:10.1242/dmm.000117
Palmieri, N., Kosiol, C. and Schlötterer, C. (2014). The life cycle of Drosophila orphan genes. *eLife* **3**, e01311. doi:10.7554/eLife.01311
Peiris, T. H., Weckerle, F., Ozamoto, E., Ramirez, D., Davidian, D., Garcia-Ojeda, M. E. and Oviedo, N. J. (2012). TOR signaling regulates planarian stem cells and controls localized and organismal growth. *J. Cell Sci.* **125**, 1657-1665. doi:10.1242/jcs.104711
Peiris, T. H., Ramirez, D., Barghouth, P. G. and Oviedo, N. J. (2016). The Akt signaling pathway is required for tissue maintenance and regeneration in planarians. *BMC Dev. Biol.* **16**, 7. doi:10.1186/s12861-016-0107-z
Pellettieri, J., Fitzgerald, P., Watanabe, S., Mancuso, J., Green, D. R. and Sánchez Alvarado, A. (2010). Cell death and tissue remodeling in planarian regeneration. *Dev. Biol.* **338**, 76-85. doi:10.1016/j.ydbio.2009.09.015
Pifferi, F. and Aujard, F. (2019). Caloric restriction, longevity and aging: Recent contributions from human and non-human primate studies. *Prog. Neuropsychopharmacol. Biol. Psychiatry* **95**, 109702. doi:10.1016/j.pnpbp.2019.109702
Plass, M., Solana, J., Wolf, F. A., Ayoub, S., Misios, A., Glažar, P., Obermayer, B., Theis, F. J., Kocks, C. and Rajewsky, N. (2018). Cell type atlas and lineage tree of a whole complex animal by single-cell transcriptomics. *Science* **360**, eaaq1723. doi:10.1126/science.aaq1723
Pomerantz, J. H. and Blau, H. M. (2013). Tumor suppressors: enhancers or suppressors of regeneration? *Development* **140**, 2502-2512. doi:10.1242/dev.084210
Reinhardt, J. A., Wanjiru, B. M., Brant, A. T., Saelao, P., Begun, D. J. and Jones, C. D. (2013). De Novo ORFs in drosophila are important to organismal fitness and evolved rapidly from previously non-coding sequences. *PLoS Genet.* **9**, 1003860. doi:10.1371/journal.pgen.1003860
Robinson, J. T., Thorvaldsdóttir, H., Winckler, W., Guttman, M., Lander, E. S., Getz, G. and Mesirov, J. P. (2011). Integrative genomics viewer. *Nat. Biotechnol.* **29**, 24-26. doi:10.1038/nbt.1754
Ross, K. G., Omuro, K. C., Taylor, M. R., Munday, R. K., Hubert, A., King, R. S. and Zayas, R. M. (2015). Novel monoclonal antibodies to study tissue regeneration in planarians. *BMC Dev. Biol.* **15**, 2. doi:10.1186/s12861-014-0050-9
Salazar-Roa, M. and Malumbres, M. (2017). Fueling the cell division cycle. *Trends Cell Biol.* **27**, 69-81. doi:10.1016/j.tcb.2016.08.009
Sanchez Alvarado, A. and Newmark, P. A. (1999). Double-stranded RNA specifically disrupts gene expression during planarian regeneration. *Proc. Natl Acad. Sci. USA* **96**, 5049-5054. doi:10.1073/pnas.96.9.5049
Saxton, R. A. and Sabatini, D. M. (2017). mTOR signaling in growth, metabolism, and disease. *Cell* **168**, 960-976. doi:10.1016/j.cell.2017.02.004
Schlötterer, C. (2015). Genes from scratch - the evolutionary fate of de novo genes. *Trends Genet.* **31**, 215-219. doi:10.1016/j.tig.2015.02.007
Solana, J., Kao, D., Mihaylova, Y., Jaber-Hijazi, F., Malla, S., Wilson, R. and Aboobaker, A. (2012). Defining the molecular profile of planarian pluripotent stem cells using a combinatorial RNAseq, RNA interference and irradiation approach. *Genome Biol.* **13**, R19. doi:10.1186/gb-2012-13-3-r19
Sureda-Gómez, M., Martín-Durán, J. M. and Adell, T. (2016). Localization of planarian β-CATENIN-1 reveals multiple roles during anterior-posterior regeneration and organogenesis. *Development* **143**, 4149-4160. doi:10.1242/dev.135152
Tautz, D. and Domazet-Lošo, T. (2011). The evolutionary origin of orphan genes. *Nat. Rev. Genet.* **12**, 692-702. doi:10.1038/nrg3053
Thommen, A., Werner, S., Frank, O., Philipp, J., Knittelfelder, O., Quek, Y., Fahmy, K., Shevchenko, A., Friedrich, B. M., Jülicher, F. et al. (2019). Body size-dependent energy storage causes Kleiber's law scaling of the metabolic rate in planarians. *eLife* **8**, 1-29. doi:10.7554/eLife.38187
Toll-Riera, M., Bosch, N., Bellora, N., Castelo, R., Armengol, L., Estivill, X. and Mar Alba, M. (2009). Origin of primate orphan genes: a comparative genomics approach. *Mol. Biol. Evol.* **26**, 603-612. doi:10.1093/molbev/msn281
Trifinopoulos, J., Nguyen, L.-T., von Haeseler, A. and Minh, B. Q. (2016). W-IQ-TREE: a fast online phylogenetic tool for maximum likelihood analysis. *Nucleic Acids Res.* **44**, W232-W235. doi:10.1093/nar/gkw256
Tu, K. C., Pearson, B. J. and Sánchez Alvarado, A. (2012). TORC1 is required to balance cell proliferation and cell death in planarians. *Dev. Biol.* **365**, 458-469. doi:10.1016/j.ydbio.2012.03.010
Tumaneng, K., Schlegelmilch, K., Russell, R. C., Yimlamai, D., Basnet, H., Mahadevan, N., Fitamant, J., Bardeesy, N., Camargo, F. D. and Guan, K.-L. (2012). YAP mediates crosstalk between the Hippo and PI(3)K-TOR pathways by suppressing PTEN via miR-29. *Nat. Cell Biol.* **14**, 1322-1329. doi:10.1038/ncb2615
Van Oss, S. B. and Carvunis, A. R. (2019). De novo gene birth. *PLoS Genet.* **15**, e1008160. doi:10.1371/journal.pgen.1008160
Udan, R. S., Kango-Singh, M., Nolo, R., Tao, C. and Halder, G. (2003). Hippo promotes proliferation arrest and apoptosis in the Salvador/Warts pathway. *Nat. Cell Biol.* **5**, 914-920. doi:10.1038/ncb1050
Waterhouse, A. M., Procter, J. B., Martin, D. M. A., Clamp, M. and Barton, G. J. (2009). Jalview Version 2–a multiple sequence alignment editor and analysis workbench. *Bioinformatics* **25**, 1189-1191. doi:10.1093/bioinformatics/btp033
Wenemoser, D. and Reddien, P. W. (2010). Planarian regeneration involves distinct stem cell responses to wounds and tissue absence. *Dev. Biol.* **344**, 979-991. doi:10.1016/j.ydbio.2010.06.017
Wenemoser, D., Lapan, S. W., Wilkinson, A. W., Bell, G. W. and Reddien, P. W. (2012). A molecular wound response program associated with regeneration initiation in planarians. *Genes Dev.* **26**, 988-1002. doi:10.1101/gad.187377.112
Werner, M. S., Sieriebriennikov, B., Prabh, N., Loschko, T., Lanz, C. and Sommer, R. J. (2018). Young genes have distinct gene structure, epigenetic profiles, and transcriptional regulation. *Genome Res.* **28**, 1675-1687. doi:10.1101/gr.234872.118
Willsey, H. R., Zheng, X., Carlos Pastor-Pareja, J., Willsey, A. J., Beachy, P. A. and Xu, T. (2016). Localized JNK signaling regulates organ size during development. *eLife* **5**, 1-18. doi:10.7554/eLife.11491
Wilson, G. A., Bertrand, N., Patel, Y., Hughes, J. B., Feil, E. J. and Field, D. (2005). Orphans as taxonomically restricted and ecologically important genes. *Microbiology* **151**, 2499-2501. doi:10.1099/mic.0.28146-0
Wilson, B. A., Foy, S. G., Neme, R. and Masel, J. (2017). Young genes are highly disordered as predicted by the preadaptation hypothesis of de novo gene birth. *Nat. Ecol. Evol.* **1**, 0146. doi:10.1038/s41559-017-0146
Wolfson, R. L. and Sabatini, D. M. (2017). The dawn of the age of amino acid sensors for the mTORC1 Pathway. *Cell Metab.* **26**, 301-309. doi:10.1016/j.cmet.2017.07.001
Yoon, M. S. (2017). The role of mammalian target of rapamycin (mTOR) in insulin signaling. *Nutrients* **9**, E1176. doi:10.3390/nu9111176
Zeng, Q. and Hong, W. (2008). The emerging role of the hippo pathway in cell contact inhibition, organ size control, and cancer development in mammals. *Cancer Cell* **13**, 188-192. doi:10.1016/j.ccr.2008.02.011
Zhao, L., Saelao, P., Jones, C. D. and Begun, D. J. (2014). Origin and spread of de novo genes in Drosophila melanogaster populations. *Science* **343**, 769-772. doi:10.1126/science.1248286